



MICROMETEOROLOGY GROUP
University of Bayreuth

BACHELOR THESIS

**Trends of Climatological Frost
Indices in Different Types of
Landscape: a Case Study in
Northern Bavaria**

Inke Grosche

Supervision

Dr. Wolfgang Babel

February, 2020

Declaration of Authorship

I declare that I completed this thesis on my own and that information which has been directly or indirectly taken from other sources has been noted as such. Neither this nor a similar work has been presented to an examination committee.

Ort, Datum

Vorname, Nachname

Acknowledgements

I would like to thank everyone, who contributed to this bachelor thesis.

Special thanks go to my supervisor Dr. Wolfgang Babel, for the professional advice, the support in R, and the valuable discussions.

Furthermore, I would like to thank Professor Dr. Christoph Thomas for the opportunity to write this thesis and for the feedback during the seminar and group meetings.

Additional thanks go to my family and friends for all the support and encouragement.

Abstract

Since the beginning of the 20th century, the global mean temperature is rising. This rise is caused by the anthropogenic greenhouse effect. However, this trend can be spatially and seasonally different. Nevertheless, even on a regional scale increases are observed, especially at low temperatures and especially in winter and early spring. These increases in temperature have an influence on the climatological frost indices.

This bachelor thesis aims to discover possibly occurring changes and trends in the climatological frost indices at a local scale, to compare them between three different sites and to make a statement regarding the possible shift of the frost risk.

The last decades are examined to find out how the trends discovered in the climatological frost indices since the beginning of the 20th century develop. Based on the literature research, a decrease in the number of frost and ice days per winter year and an increase of the mean frost period temperature and the minimum temperature as well as a delay trend of the first frost day and an advanced occurrence of the last frost day were expected.

Some of these expectations were confirmed by the data analysis. A few significant trends were identified which are however occurring spatially heterogeneous at the three stations.

The results of the analysis differ between the three measuring stations. These differences are consistent with expected deviations caused by microclimate at the sites. The influence of cold-air drainage, as well as the influence of the spruce forest appear at the respective sites.

The occurrence of phenological spring events is advancing for most of the investigated plants at one of two examined sites. However, the results of the frost risk analysis were contradictory for the two examined sites. The frost risk appears to stagnate at one site, whereas it seems to decrease at the other site.

The findings of this study are limited by the short measuring time of the meteorological stations and the partly large data gaps as well as the distance between the meteorological and phenological stations. So, these results can not be confirmed with absolute certainty.

Nevertheless, these findings can give an insight on how climatological frost indices are changing and an impulse for future research to discover in more detail, how these indices are developing under future global climate change.

Zusammenfassung

Seit Beginn des 20. Jahrhunderts steigen weltweit die mittleren Temperaturen an, verursacht durch den anthropogenen Treibhauseffekt. Dieser Trend kann jedoch räumlich und saisonal unterschiedlich sein. Allerdings kommt es auch auf regionaler Skala zu Anstiegen insbesondere der Minimumtemperatur, verstärkt im Winter und Frühjahr. Dieser Anstieg der Temperatur wirkt sich auf die Frostkenntage aus.

Das Ziel der vorliegenden Bachelorarbeit ist es, in den Frostkenntagen möglicherweise auftretende zeitliche Veränderungen und Trends zu entdecken, diese zwischen den drei verschiedenen Stationen zu vergleichen und eine Aussage bezüglich der möglichen Verschiebung des Frostrisikos zu machen.

Betrachtet werden die letzten Dekaden, um herauszufinden, wie sich die entdeckten Trends in den Frostkenntagen seit Beginn des 20. Jahrhunderts entwickeln. Aufgrund der Literaturrecherche wurde eine Abnahme der Frosttage und Eistage pro Winterjahr erwartet. Des weiteren wurde mit einem Anstieg der mittleren Frostperiodentemperatur und der Minimumtemperatur sowie einer Verschiebung des ersten Frosttages nach hinten und des letzten Frosttages hin zu früherem Eintreten gerechnet.

Einige dieser Erwartungen konnten durch die Analyse bestätigt werden. Ein paar signifikante Trends konnte festgestellt werden, die sich jedoch sehr unterschiedlich an den drei Stationen zeigen.

Die Ergebnisse der Analyse unterscheiden sich zwischen den drei Messstationen. Diese Unterschiede entsprechen den erwarteten Abweichungen, verursacht durch die mikroklimatische Situation der Standorte. Der Einfluss des Kaltluftabflusses, sowie der Einfluss des Nadelwaldes zeigen sich an den jeweiligen Standorten.

Phänologische Frühlingsevents treten bei den meisten untersuchten Pflanzen immer früher auf bei einem von zwei untersuchten Standorten. Es zeigt sich bezüglich des Frostrisikos jedoch für die beiden Standorte ein gegensätzliches Bild, da an einem Standort das Frostrisiko zu stagnieren scheint, während an dem anderen Standort das Frostrisiko zu sinken scheint.

Wegen der kurzen Messzeiträume der meteorologischen Stationen und den teilweise großen Datenlücken, sowie der räumlichen Distanz zwischen den meteorologischen und phänologischen Stationen, können diese Ergebnisse jedoch nicht mit letzter Sicherheit bestätigt werden.

Trotzdem können diese Ergebnisse einen Einblick geben, wie sich Frostkenntage verändern und einen Anstoß für zukünftige Forschung geben, genauer zu untersuchen, wie sich diese Kenntage infolge des globalen Klimawandels entwickeln.

Contents

Declaration of Authorship	I
Acknowledgements	II
Abstract	III
Zusammenfassung	IV
Contents	V
List of Figures	VII
List of Tables	XIV
1 Introduction	1
2 Material and Methods	9
2.1 Measuring Stations	9
2.2 Measuring Instruments	11
2.3 Data Analysis with R	12
2.4 Pre-Analysis: Data Gaps	13
3 Results	18
3.1 Annual Course and Distribution of the Daily Temperature	18
3.2 Winter Indices	21
3.2.1 Mean Frost Period Temperature and Coldest Day	21
3.2.2 Frost and Ice Days	24
3.2.3 First and Last Frost Day	27
3.2.4 Frost-free Period	30
3.2.5 Interrelationships among Indices and Comparison to regional trends	31
3.3 Frost Event based Statistics	36
3.3.1 The number of Frost and Ice Events	36
3.3.2 Mean Event Length	38
3.3.3 Maximum continuous ice event	40
3.4 Comparison of the annual frost statistics with phenological events	41
3.4.1 Trends in the Phenological Spring Data	41
3.4.2 Comparison of the vegetation period	44
3.4.3 Frost Risk Analysis	47
4 Discussion	50

5 Conclusion	59
Bibliography	60
Appendix	63

List of Figures

- 1 Increase of the atmospheric CO₂ concentration at Mauna Loa Observatory between 1960 and 2019. The red line represents the monthly mean values, the black line the monthly mean values after correction for the averaged seasonal cycle. Image provided by NOAA ESRL Global Monitoring Division, Boulder, Colorado, USA (<http://esrl.noaa.gov/gmd/ccgg/trends/>) 1
- 2 Radiation balance of the Earth with the shortwave radiation (global radiation and reflected radiation) in yellow fluxes and the longwave radiation (surface radiation and back radiation) in red fluxes. The processes are written in white/blue, greenhouse gases are shown as a green layer. The energy flux is given in the numbers in the unit Wm⁻². Image from CERES, NASA, (https://ceres.larc.nasa.gov/ceres_brochure.php?page=2) . 2
- 3 Increase in the global annual mean temperature anomalies, relative to 1951-1980 average temperatures. Slow increase from 1910 - 1940, intervening period around 1940 - 1975, accelerated increase since 1975. Grey lines with points: annual mean, black line: lowess smoothing. Image provided by NASA (<https://climate.nasa.gov/vital-signs/global-temperature/>) 3
- 4 Decrease of the frost days over large parts of the Northern Hemisphere. The trend rate is represented by the color, significant trends are bordered with black (Kiktev et al., 2003) 4
- 5 Last spring (-2.2°C) frost date departure by year across the Northern Hemisphere, 1955 - 2002. A linear regression trend is shown with a black dashed line. (Schwartz et al., 2006) 5
- 6 Position of the measuring stations in the vicinity of Bayreuth. The measuring stations are marked with red (EBG), green (Voitsumra) and yellow (Waldstein). Image provided by the Micrometeorology Group, University Bayreuth, (http://www.bayceer.uni-bayreuth.de/meteo/de/klima/gru/html.php?id_obj=139706) 9
- 7 Hovmöller plots of the daily 2m height HMP45 temperature date at the EBG, Voitsumra and Waldstein. Days with valuable data are shown in grey, days with more than 10% missing data are shown in white. At the EBG a large data gap occurs in winter year 2015 and 2016, the most data gaps occur at the Voitsumra site. 14
- 8 Temperature measured at 2m height in February 2018 with the HMP45 (blue) and the Psychrometer (red) at the EBG station 15
- 9 Scatterplot of the aggregated mean, minimum and maximum temperature data measured with the HMP45 against measured with the Psychrometer at the EBG station. A line of equality (x=y line) is shown additionally. . 15

10	Scatterplot of the mean frost period temperature measured with the HMP45 versus measured with the Psychrometer, EBG. A linear regression line is plotted in blue, a line of equality ($x=y$ line) in red.	16
11	Scatterplot of the number of frost days measured with the HMP45 versus measured with the Psychrometer, EBG. A linear regression line is plotted in blue, a line of equality ($x=y$ line) in red.	17
12	Hovmöller plot of the daily minimum temperature data, EBG. All frost days (T_{\min} below 0°C) are depicted in blue. The mean first and last frost days are shown with two black lines. Data gaps are shown in white.	18
13	Histograms of the daily minimum and the daily maximum temperature at the EBG site, for the period 1999 – 2008 (red) and the period 2009 - 2018 (blue)	19
14	Histograms of the daily minimum and the daily maximum temperature at the Voitsumra site, for the period 1999 – 2008 (red) and the period 2009 - 2018 (blue)	20
15	Histograms of the daily minimum and the daily maximum temperature at the Waldstein site, for the period 1999 - 2008 (red) and the period 2009 - 2018 (blue)	20
16	Comparison of the mean frost period temperature between the three station. The Waldstein station is shown in black, the Voitsumra station in blue and the EBG station in green. A linear regression line is depicted for the Waldstein results, as there occurs a significant trend.	21
17	Minimum temperature per winter year at the EBG site. The minimum temperature at 2 m height is shown in black, at 5 cm height in red.	22
18	Date of the minimum temperature per winter year in the EBG. For the 2 m height measurement shown in black, for the 5 cm height in red.	23
19	Comparison of the minimum temperature per winter at the three stations. The Waldstein station is shown in black, the Voitsumra station in blue and the EBG station in green.	23
20	Comparison of the date of the minimum temperature per winter at the three stations. The Waldstein station is shown in black, the Voitsumra station in blue and the EBG station in green.	24
21	Absolute number of ice and frost days per winter, EBG. The frost days at 2 m height are shown in black, those at 5 cm height are shown in red. The ice days are depicted in blue.	24

22	Comparison of the number of frost days between the different stations. The Waldstein station is shown in black, the Voitsumra station in blue and the EBG station in green. The Bavarian average of frost days is pictured additionally in orange. A linear regression line is shown for the Waldstein site, where the number of frost days is decreasing.	25
23	Comparison of the number of ice days between the different stations. The Waldstein station is shown in black, the Voitsumra station in blue and the EBG station in green. The Bavarian average of ice days is pictured additionally in orange.	26
24	Date of the first frost day at the EBG. The 2 m height measurement is shown in black, the 5 cm height measurement in red. In winter year 2019, two dates are depicted, the one with the dashed line is the original first frost day. A linear regression line is depicted additionally, as there appears a trend in the 5 cm measurements.	27
25	Temperature course at the date of the first and second frost day, winter year 2019, EBG	28
26	Date of the last frost day at the EBG station. The 2 m height measurement is shown in black, the 5 cm height measurement in red. A linear regression line is depicted additionally, as there appears a trend in the 5 cm measurements.	28
27	Comparison of the date of the first frost day between the three stations. The Waldstein station is shown in black, the Voitsumra station in blue and the EBG station in green.	29
28	Comparison of the date of the last frost day between the three stations. The Waldstein station is shown in black, the Voitsumra station in blue and the EBG station in green. A linear regression line is shown additionally for the Voitsumra station, as there occurs a significant negative trend.	29
29	Number of days of the frost-free period at the EBG station. The 2 m height measurement is shown in black, the 5 cm height measurement in red. A linear regression line is depicted additionally, as there appears a significant trend in the 5 cm measurements.	30
30	Comparison of the length of the frost-free period between the three stations. The Waldstein station is shown in black, the Voitsumra station in blue and the EBG station in green.	31
31	Scatterplot of the the number of frost days versus mean frost period temperature at the EBG, Voitsumra and Waldstein site. A linear regression line is shown additionally in red.	32

32	Absolute number of frost days for Bavaria (blue) and Germany (yellow). For both, a linear regression line is shown additionally, as there appear significant trends. Data provided by the German meteorological service (https://opendata.dwd.de/climate_environment/CDC/regional_averages_DE/annual/frost_days/)	34
33	Scatterplots of the frost days measured at the meteorological stations versus the Bavarian average. A linear regression line is depicted in blue, a line of equality (x=y line) in red.	34
34	Absolute number of ice days for Bavaria (blue) and Germany (yellow). For both, a linear regression line is shown additionally, as there appear significant trends. Data provided by the German meteorological service (https://opendata.dwd.de/climate_environment/CDC/regional_averages_DE/annual/ice_days/)	35
35	Scatterplot of the number of ice days of the three stations versus the Bavarian average. A linear regression line is depicted in blue, a line of equality (x=y line) in red.	36
36	Absolute number of ice and frost events per winter in the EBG. The frost events at 2 m height are shown in black, those at 5 cm height are shown in red. The ice events are depicted in blue.	37
37	Comparison of the number of frost events between the three stations. The Waldstein station is shown in black, the Voitsumra station in blue and the EBG station in green.	37
38	Comparison of the number of ice events between the three stations. The Waldstein station is shown in black, the Voitsumra station in blue and the EBG station in green.	38
39	Mean frost event length in days per event at the EBG site. The mean frost event length at 2 m height are shown in black, those at 5 cm height is shown in red.	38
40	Comparison of the mean frost event length in days per event between the three stations. The Waldstein station is shown in black, the Voitsumra station in blue and the EBG station in green.	39
41	Comparison of the mean ice event length in days per event between the three stations. The Waldstein station is shown in black, the Voitsumra station in blue and the EBG station in green.	39
42	Comparison of the maximum continuous ice events in days per event between the three stations. The Waldstein station is shown in black, the Voitsumra station in blue and the EBG station in green.	40

43	Date of the bud break begin and of the leaf unfolding begin of the mountain ash (Eberesche) at the site Weißenstadt. The bud break begin is shown in green, the leaf unfolding begin in blue. A linear regression line for the bud break begin is plotted additionally, as there occurs a significant trend. Data provided by the German Meteorological Service (https://opendata.dwd.de/climate_environment/CDC/observations_germany/phenology/annual_reporters/wild/historical/)	41
44	Date of the leaf unfolding begin of the copper beech (Rotbuche) at the site Weißenstadt. A linear regression line is plotted additionally, as there occur a significant trend. Data provided by the German Meteorological Service (https://opendata.dwd.de/climate_environment/CDC/observations_germany/phenology/annual_reporters/wild/historical/)	42
45	Date of the blooming begin of the mountain ash (Eberesche) at the site Weißenstadt. A linear regression line is plotted additionally, as there occurs a significant trend. Data provided by the German Meteorological Service (https://opendata.dwd.de/climate_environment/CDC/observations_germany/phenology/annual_reporters/wild/historical/)	43
46	Date of the blooming begin of the coltsfoot (Hufflattich) at the site Weißenstadt. A linear regression line is plotted additionally, as there occurs a significant trend. Data provided by the German Meteorological Service (https://opendata.dwd.de/climate_environment/CDC/observations_germany/phenology/annual_reporters/wild/historical/)	43
47	Comparison of the main vegetation period length between the three stations. The Waldstein station is shown in black, the Voitsumra station in blue and the EBG station in green. A linear regression line is shown additionally for the Waldstein station, as there occurs a significant trend. .	44
48	Start of the main vegetation period between the three stations. The Waldstein station is shown in black, the Voitsumra station in blue and the EBG station in green. A linear regression line is shown additionally for the Waldstein station, as there occurs a significant trend.	45
49	Comparison of the growing season length and the main vegetation period length at the EBG station. The growing season length is shown in light turquoise, the main vegetation period length in dark turquoise.	46

50	Comparison of the growing season length and the main vegetation period length with the phenological vegetation period at the Voitsumra/Weißenstadt site. The growing season length is shown in light turquoise, the main vegetation period length in dark turquoise. The phenological vegetation period of the mountain ash (Eberesche) is shown in green and those of the copper beech (Rotbuche) in orange. Phenological data provided by the German Meteorological Service (https://opendata.dwd.de/climate_environment/CDC/observations_germany/phenology/annual_reporters/wild/historical/)	46
51	Phenological spring data of the mountain ash at the Aichig site and the last frost day at the EBG station. The last frost day is depicted in light blue, the bud break begin in green, the leaf unfolding begin in dark blue and the blooming begin in orange. Phenological data provided by the German meteorological service (https://opendata.dwd.de/climate_environment/CDC/observations_germany/phenology/annual_reporters/wild/historical/)	47
52	Phenological spring data of the mountain ash at the Weißenstadt station and the last frost day at the Voitsumra station. The last frost day is depicted in light blue, the bud break begin in green, the leaf unfolding begin in dark blue and the blooming begin in orange. Phenological data provided by the German meteorological service (https://opendata.dwd.de/climate_environment/CDC/observations_germany/phenology/annual_reporters/wild/historical/)	48
53	Daily Aggregated Temperature Data at 2 m height at the EBG Site over the entire measuring Period, measured with the HMP 45. The Daily Mean Temperature is shown in black, the Daily Minimum Temperature in blue and the Daily Maximum Temperature in red.	63
54	Daily Aggregated Temperature Data at 2 m height at the Voitsumra Site over the entire measuring Period, measured with the HMP 45. The Daily Mean Temperature is shown in black, the Daily Minimum Temperature in blue and the Daily Maximum Temperature in red.	63
55	Daily Aggregated Temperature Data at 2 m height at the Waldstein Container Station over the entire measuring Period, measured with the HMP 45. The Daily Mean Temperature is shown in black, the Daily Minimum Temperature in blue and the Daily Maximum Temperature in red.	64
56	Daily Aggregated Temperature Data at 2 m height at the Waldstein Tower Station over the entire measuring Period, measured with the HMP 45. The Daily Mean Temperature is shown in black, the Daily Minimum Temperature in blue and the Daily Maximum Temperature in red.	64

57	Hovmöller Plot of the Daily Minimum Temperature Data at the Voitsurma Station. All Frost Days (T_{\min} below 0°C) are depicted in blue. The Mean First and Last Frost Days are shown with two black Lines. Data Gaps are shown in white.	64
58	Hovmöller Plot of the Daily Minimum Temperature Data at the Voitsurma Station. All Frost Days (T_{\min} below 0°C) are depicted in blue. The Mean First and Last Frost Days are shown with two black Lines. Data Gaps are shown in white.	65
59	Scatterplot of the the Number of Ice Days versus Mean Frost Period Temperature at the EBG, Voitsumra and Waldstein site. A Linear Regression Line is shown additionally in red. The results of the Correlation Analysis and the Linear Equation are shown in the graphic.	65

List of Tables

1	Summary of the climatological frost indices, their calculation and unit . . .	13
2	Summary table of the discovered correlations between climatological frost indices. The correlation coefficient is mentioned with the respective p-value in parenthesis. The rate of the linear regression is mentioned as well, otherwise "NA" is written.	33
3	Summary table of the discovered trends at the measurement sites. Unit is "days per decade" unless otherwise noted. Trends significant at a 95% level of confidence are mentioned in bold. Non significant trends are mentioned with the respective p-value in parenthesis. If no trend appeared, "/" is written. Trends in the 5cm measurement of the EBG are mentioned in parenthesis.	53
4	Summary table of the expected and discovered trends in the phenological data at the Weißenstadt station. Unit of trends is "days per decade" unless otherwise noted. Trends significant at a 95% level of confidence are mentioned in bold. Non significant trends are mentioned with the respective p-value in parenthesis. If no trend appeared, "/" is written. If the indices is not measured or not calculated "NA" is pictured.	56

1 Introduction

Humans influence the climate in many ways. Through changing the way the land is used they have brought about alterations in the heat and energy balance. The water regime and especially the chemical composition of the atmosphere have also been impacted by human actions (Schönwiese, 2013). This influence can be seen in the continuing climate change. The global climate system is largely influenced by the concentration of greenhouse gases in the atmosphere. The main effective greenhouse gases are CO_2 (Carbon dioxide), CH_4 (Methane) and N_2O (Nitrous Oxide) (Schönwiese, 2013). The concentration of all these three greenhouse gases has increased during in the last decades. The longest record of atmospheric CO_2 concentrations began in 1958 at the observatory of the Mauna Loa (Hawaii, station at 3397m) and is shown in Figure 1.

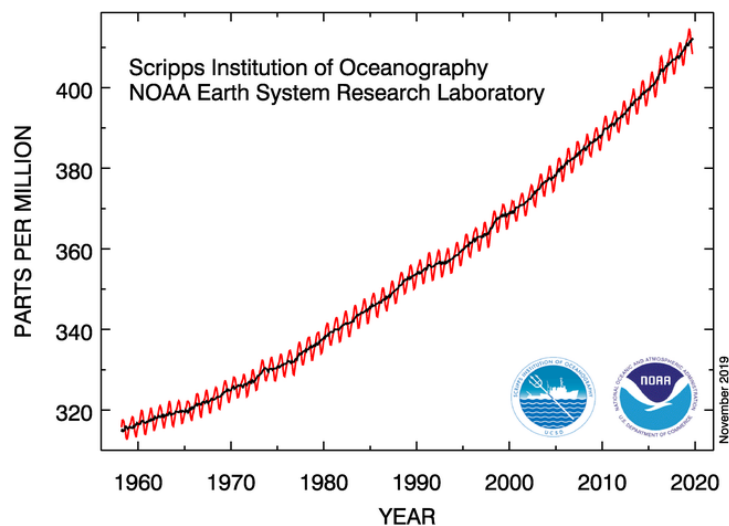


Figure 1: Increase of the atmospheric CO_2 concentration at Mauna Loa Observatory between 1960 and 2019. The red line represents the monthly mean values, the black line the monthly mean values after correction for the averaged seasonal cycle. Image provided by NOAA ESRL Global Monitoring Division, Boulder, Colorado, USA (<http://esrl.noaa.gov/gmd/ccgg/trends/>)

Since 1960, a constant increase of the concentration of atmospheric CO_2 is recorded at the Mauna Loa Observatory. In September 2019, the concentration reached 408.54 ppm (NOAA ESRL). Through these measurement and through indirect reconstructions, a first slow and then accelerated increase in the concentration of CO_2 can be observed. The concentration of greenhouse gases is affecting the radiation balance of the earth system.

The radiation balance of the earth is shown in figure 2. The yellow schematic fluxes with the red arrows are illustrating the shortwave radiation, or more specific the incoming solar radiation (global radiation) and the reflected solar radiation. A part of the shortwave incoming solar radiation is absorbed at the earth surface. The earth heats up and emits longwave radiation. The effect of CO_2 and the other greenhouse gases is visible in the

energy flux of the long-wave radiation.

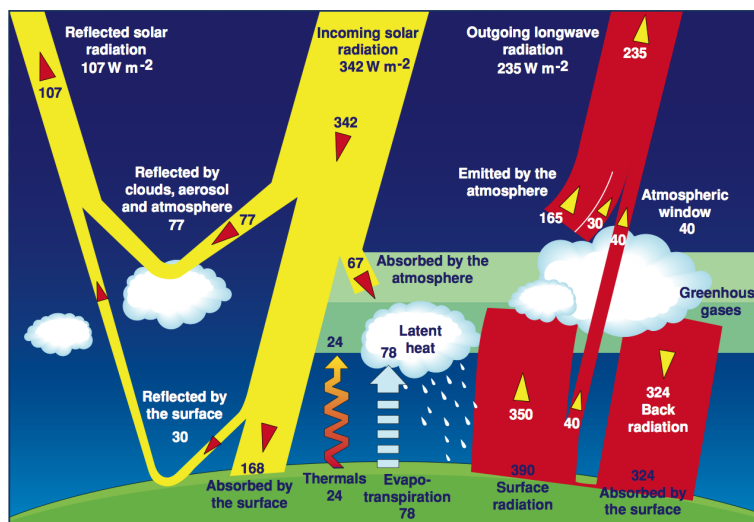
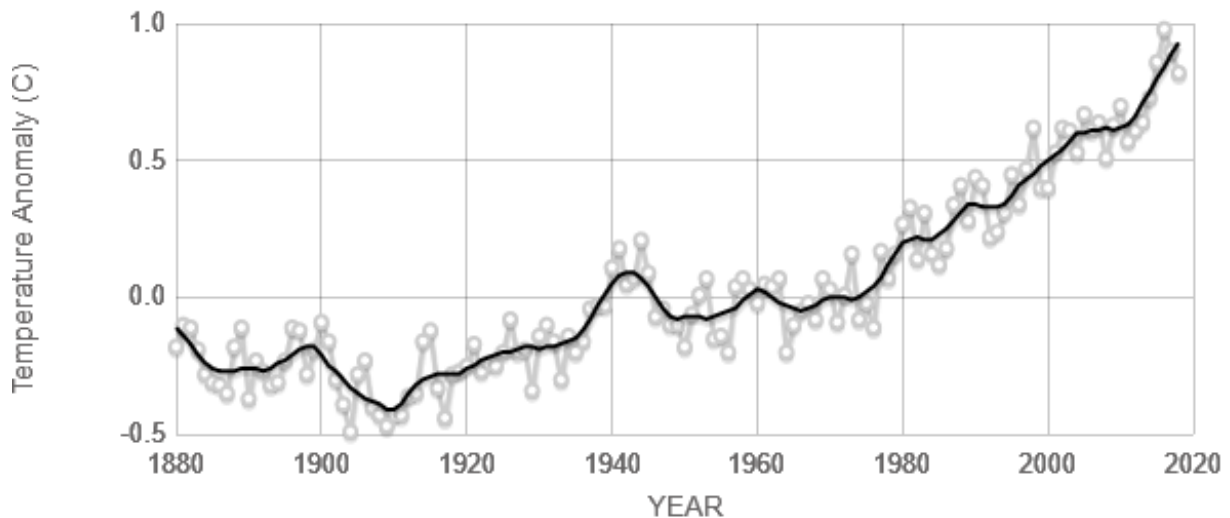


Figure 2: Radiation balance of the Earth with the shortwave radiation (global radiation and reflected radiation) in yellow fluxes and the longwave radiation (surface radiation and back radiation) in red fluxes. The processes are written in white/blue, greenhouse gases are shown as a green layer. The energy flux is given in the numbers in the unit Wm^{-2} . Image from CERES, NASA, (https://ceres.larc.nasa.gov/ceres_brochure.php?page=2)

The surface radiation is represented by the red flux with yellow arrows going to the space. A large part of this radiation is reflected, absorbed and re-emitted by the greenhouse gases. This large part is going back to the earth surface as back radiation (second red flux). The amount of longwave incoming radiation (back radiation) increases as the concentration of greenhouse gases increases. Thus, the amount of energy in the earth system is increasing. As a result, an increase in the global mean air temperature has been observed since the beginning of the 20th century. With consideration of the possible natural and anthropogenic drives, the anthropogenic trend rate is around 0.6 - 0.7 K with an uncertainty of about ± 0.2 K in the last century. If just the effect of the greenhouse gases are considered, a trend of about 1 K appears (Schönwiese, 2013). Jones and Moberg (2003) discovered a warming of 0.07 K per decade in the period from 1901 to 2000 (highly significant trend). This warming is not continuous but takes place mainly in two periods, the first from 1920 to 1945 and the second since 1975.

The global temperature anomalies of the last 140 years, relative to the average of 1951 - 1980, are shown in figure 3. Since around 1910 the global mean temperature is increasing all in all continuously with an intervening period around 1940 - 1975. Nevertheless, the temperature trends vary strongly over time (year after year), seasonally and spatially (Jones and Moberg, 2003). According to general expectations, the global temperature is likely to rise further. It is expected to rise by up to 5.8°C before the end of the 21th century (Rochette et al., 2004).



Source: climate.nasa.gov

Figure 3: Increase in the global annual mean temperature anomalies, relative to 1951-1980 average temperatures. Slow increase from 1910 - 1940, intervening period around 1940 - 1975, accelerated increase since 1975. Grey lines with points: annual mean, black line: lowess smoothing. Image provided by NASA (<https://climate.nasa.gov/vital-signs/global-temperature/>)

However, climate change is not only reflected in global annual averages, but also in extreme values. A significant increase in the daily minimum temperature in winter between 1900 and 1998 was observed in Bonsal et al. (2001), along with a significant trend towards fewer days with extremely low temperatures in winter, spring and summer. In particular, they discovered a stronger increase in minimum temperatures than in maximum temperatures. Thus, the change in temperatures is greater in winter and early spring than in other seasons. This assumption is supported by Sparks and Menzel (2002), who described that temperature changes were more pronounced in winter and early spring than in the other seasons.

This change of temperatures in winter and spring is reflected in several indices like the number of frost days, the first and the last frost day and the frost-free period. The number of frost days is a parameter to quantify the number of days with a minimum temperature below 0°C . At these days, the low temperature can cause damage of plants. The first and last frost day are therefore marking the potential start and end of the frost risk free growing season. Therefore, the frost-free period is a value for the length of the potential growing season. In this period, growing with no frost risk is possible. According to Frich et al. (2002), the number of frost days per winter are decreasing significantly at a global scale over the second part of the 20th century. These findings are supported by Kiktev et al. (2003) who found locally significant decreases in the number of frost days during the period 1950 - 1995 across Central Europe (see in figure 4). In Canada, a significant

decrease in the frequency of spring frost (number of days minimum temperature falls below 0°C) was discovered between 1900 and 1998 (Bonsal et al., 2001).

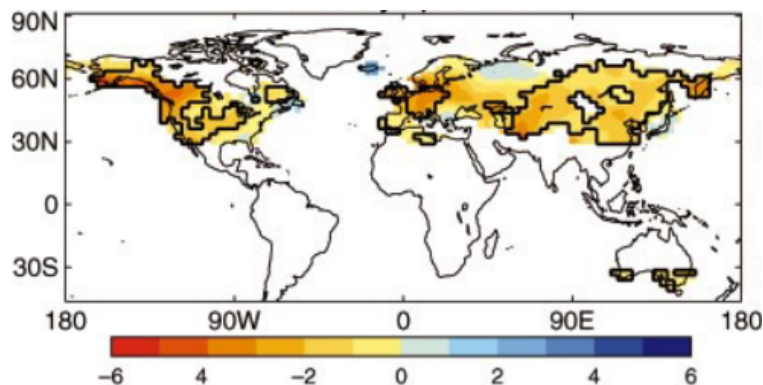


Figure 4: Decrease of the frost days over large parts of the Northern Hemisphere. The trend rate is represented by the color, significant trends are bordered with black (Kiktev et al., 2003)

These trends are reflected in the highly significant decrease of snow days per winter over the last 60 years, which has further accelerated the last 15 years (Kreyling and Henry, 2011). Additionally, the length of the frost-free period (period during which the daily minimum temperature is constantly above 0°C) is increasing significantly for most of Canada, according to Bonsal et al. (2001). This lengthening is due to a significant earlier start, specifically an advancing last frost day. Likewise, the later end, specifically a later occurring first frost day, result in the lengthening, with a minor influence. These findings are supported by Schwartz et al. (2006). They observed an increase of the frost-free period as well, mainly driven by earlier last frost dates in spring (rate of 1,5 days per decade, see figure 5; Schwartz et al., 2006). A more detailed view is offered by Bigler and Bugmann (2018). Their analysis showed negative trends for the last mild to moderate spring frost ($T_{\min} < -1^{\circ}\text{C}$ to $T_{\min} < -6^{\circ}\text{C}$) particularly at elevations above 800m. To be precise, the last mild to moderate spring frost events are occurring earlier, with more pronounced trends at elevations above 800m. Meanwhile, the last severe spring frost events ($T_{\min} < -7^{\circ}\text{C}$ to $T_{\min} < 10^{\circ}\text{C}$) are shifting with positive trends, but severe spring frost occurred only in few cases during or after leaf unfolding (Bigler and Bugmann, 2018).

Another indicator linked to the temperature and important for vegetation is the thermal growing season length (period between when $T_{\text{day}} > 5^{\circ}\text{C}$ for > 5 d and $T_{\text{day}} < 5^{\circ}\text{C}$ for > 5 d). According to Frich et al. (2002) the growing season length is significantly increasing on a global scale. However, this increase is not happening at the same significance level as the decrease of the number of frost days in Europe. The lengthening of the thermal growing season length is affecting the occurrence of phenological events and phases, but not only the thermal growing season length. As described in Winkler (1980), temperature is mainly influencing plants in their life and annual cycle, and therefore, changes in temperatures are inducing a fast reply of plants. For instance, the flowering (blooming)

date of the wood anemone shows a clear response to the temperature in January to March (Sparks and Menzel, 2002).

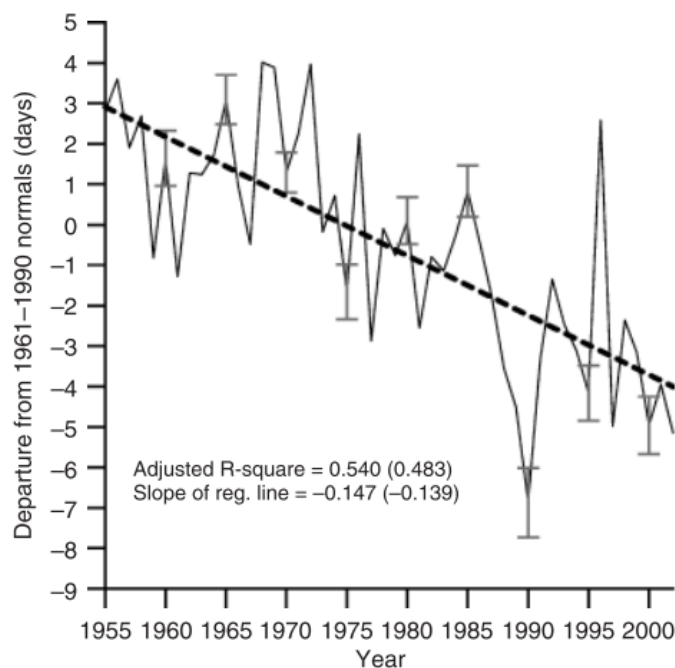


Figure 5: Last spring (-2.2°C) frost date departure by year across the Northern Hemisphere, 1955 - 2002. A linear regression trend is shown with a black dashed line. (Schwartz et al., 2006)

Generally, changing temperatures can lead to adjustments in the vegetation (Schwartz et al., 2006). As an example of an adjustment, the onset of spring events is sensitive to the temperatures in spring. Thus, it is influenced by the increase in spring temperatures due to climate change. As the temperatures are rising seasonally earlier in the year, observed spring phases of vegetation begin earlier in the year, documented by several parameters. For instance, the onset of spring events, like leaf unfolding, advanced by 6 days since the early 1960s, according to Menzel and Fabian (1999) (rate of -2.0 days per decade). This is supported by Schwartz et al. (2006), who observed that first leaf dates (for measuring 'early spring') are getting earlier with an average rate of -2.2 days per decade in Europe since 1955 and first bloom dates (for measuring 'late spring') with an average rate of -1.0 days per decade. The onset of spring events is expected to advance further by up to six days per 1 K warming (Menzel and Fabian, 1999). According to Bigler and Bugmann (2018), leaf unfolding has been advancing across all species, particularly at higher elevations above 800 m.

As the phenological spring events have advanced during the last decades, meanwhile, the begin of autumn events has delayed by 4.8 days since 1960 (Menzel and Fabian, 1999). Overall, but mainly driven by advancing spring phenologies, the growing period is extending. The period has lengthened by 10.8 days since 1960 (Menzel and Fabian,

1999). Here, the growing period is defined as the period between phenological spring events (such as leaf unfolding) and phenological autumn events (such as leaf colouring). In Chmielewski (2007), the vegetation period was observed to lengthen by 25 days in the period 1961 to 2005, as they specified the vegetation period as the period, during which the daily mean temperature is above 5°C.

Low temperatures have a twofold effect on plants: damage caused by ice formation in the cells or damage caused by desiccation, as there is no more replenishment of soil water possible (frost drought). Frost drought is occurring as there is also transpiration happening below 0°C (Winkler, 1980). Therefore, strong solar radiation in spring with low temperatures has a negative effect on plants and can cause frost damage (Winkler, 1980; Larcher, 1984). Frost resistance of vegetation is at its maximum in winter during dormancy, when the temperatures are at their lowest point. It is mainly triggered by changes in temperature and light (Menzel and Fabian, 1999). Due to the seasonal temperature rising in spring, the frost resistance of plants decreases. Thus, the frost risk increases, with the highest risk of frost damage during leaf unfolding (Bigler and Bugmann, 2018). In contrast to this, according to Schwartz et al. (2006), the potential of damage is greater, the later the last frost occurs as the plants are in a phenological more advanced phase of development. The timing of leaf unfolding is representing a trade-off between minimizing the frost risk and maximizing the growing period (Bigler and Bugmann, 2018).

However, there is little consensus whether frost risk is increasing, since advanced leaf unfolding entails an increasing frost risk. On the other hand, the last spring frost dates are advancing, as well, and climate warming leads to changes in the seasonal distribution and intensity of frost events (Bigler and Bugmann, 2018). Under future global warming, if mild spring temperatures coincide with severe spring frosts, the frost risk is likely to increase (Bigler and Bugmann, 2018). The last frost day mostly occurs after the onset of phenological spring events. If this temporal difference between the last frost event and phenological spring events is increasing, the frost risk is increasing (Schwartz et al., 2006; Scheifinger et al., 2003).

Differences in climatological frost indices among various sites can be caused by different elevations (difference of up to 400m), the impact of cold-air drainage (two sites are cold-air drainage and pooling endangered) or the influence of the vegetation (grassland vs. coniferous forest). The influence of cold-air drainage/pooling is often discovered at slight slopes in cloudless nights (strong longwave up-welling radiation) and with low to no wind. If cold-air influence arise, very low temperatures (compared to normal conditions) can occur (Foken, 2017). The influence of vegetation is caused by the different microclimatic conditions in forests compared to grassland (for instance more constant temperature under the canopy). Forests can as well be a shelter of wind or effect less low minimum temperatures due to longwave radiation of the trees.

This bachelor thesis aims to discover possible changes and trends in the climatological

frost indices at a local scale, to compare them at three different measuring sites and to make a statement regarding the possible shift of the frost risk. The research is based on two research questions. First of all, do any significant trends in the climatological frost indices like the mean frost period temperature, the minimum temperature, the number of frost and ice days or the length of the continuous ice events per winter year occur? Moreover, do significant trends emerge in the first frost day in autumn and last frost day in spring and through that the length of the frost-free period? With regard to frost risk, are there significant changes in the trends of the advancing first frost day and the advancing of the phenological spring events and is this leading to a shift in the frost risk? Second, how do the climatological frost indices (frost days, ice days, etc.) and the possibly occurring trends differ at the different measuring stations? Further, which landscape characteristics and microclimatic conditions have an impact on those and could therefore cause these differences?

In order to analyse and compare the spatial variability in the climatological frost indices and how they are altering under climate change, different types of landscapes will be considered. This is an opportunity to detect how climate change is influencing the local climate with regard to winter (and early spring) change.

Several researchers noticed changes in climatological frost indices, such as the significant decrease in the number of frost days. These researches used nearly always many stations (large scale), with available data since around 1950 (Frich et al., 2002; Kiktev et al., 2003; Schwartz et al., 2006; Chmielewski and Rötzer, 2002; Menzel et al., 2003). In contrast, this study analyses whether these trends emerge also for a shorter time series (around 20 years) and at a local scale with just three measuring stations. The three chosen stations are in the vicinity of Bayreuth. In this local scale, they have the same synoptic forcing. The differences between the stations are attributed to microclimate. At the Waldstein station, the microclimate is influenced by the nearby forest, at the Voitsumra station by the grassland and a strong cold-air drainage influence and at the EBG station by the grassland and a less strong cold-air drainage influence. The three stations are described more detailed in section 2.1.

With regard to climate change, strong winter temperature warming and based on the literature, one would expect, the number of frost days and the number of ice days is decreasing. More specific, it could be likely that the number of ice days will decrease, but it is questionable, if the frost days decrease as well, or if they are to some extent superseded by former ice days. Moreover, it is expected, that the first frost day in autumn is showing a delaying trend, while the last frost day in spring is advancing (like outlined in Menzel and Fabian (1999)). Therefore, the period with continuous temperatures above 0°C will extend. The risk of frost damage is possibly shifting, depending on the relative changes in the phenological spring events and the last frost day. For instance, the frost risk can potentially decrease, if the last frost days are advancing faster than the first phenological

spring events like ascertained in Scheifinger et al. (2003).

The three meteorological stations were chosen, as there are several local differences, but they are still near to each other. At this local scale, the synoptic forcing is similar for the stations. Climatological frost indices like the number of frost and ice days (per winter year), the number of frost and ice events, the maximum continuous ice period, the minimum temperature, the first and last frost day, but also the mean winter temperature were analyzed and examined for possibly appearing trends at three measuring sites. The number of frost and ice days was also compared to the annual mean for Bavaria and Germany. With phenological data of several plants the respective start of the phenological vegetation period was compared to the last frost days in spring. Further, the difference between these events was calculated to detect how the frost risk is developing. Additionally, the vegetation period will be calculated using various methods and possible trends will be compared with those found in the literature.

2 Material and Methods

2.1 Measuring Stations

The temperature data was collected at three meteorological measuring stations. The three meteorological stations are supervised by the Micrometeorological Group of the University of Bayreuth. In figure 6 the position of the stations is shown.

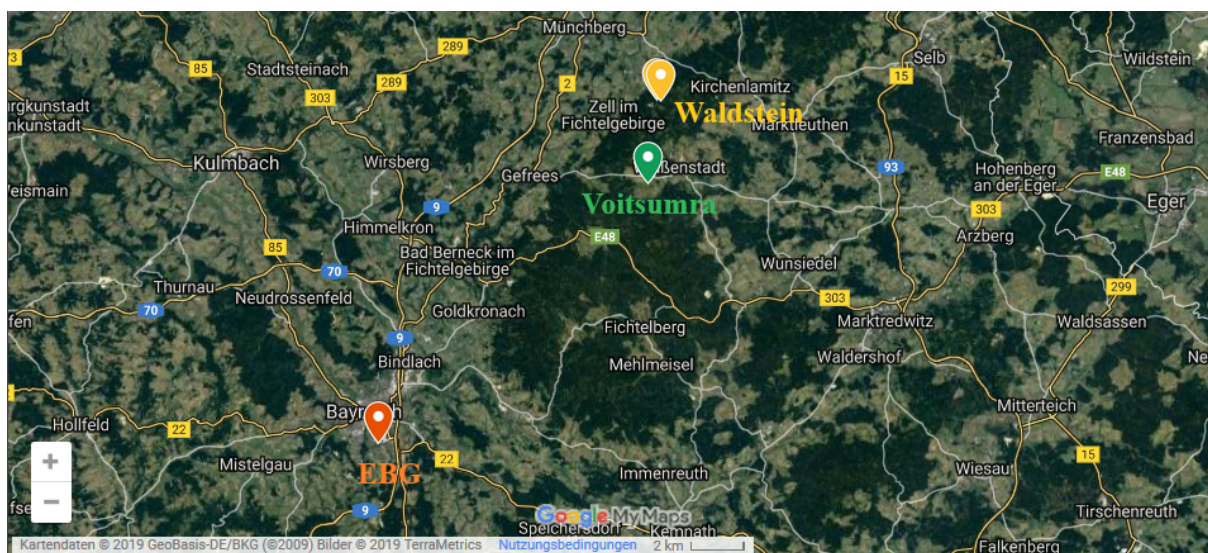


Figure 6: Position of the measuring stations in the vicinity of Bayreuth. The measuring stations are marked with red (EBG), green (Voitsumra) and yellow (Waldstein). Image provided by the Micrometeorology Group, University Bayreuth, (http://www.bayceer.uni-bayreuth.de/meteo/de/klima/gru/html.php?id_obj=139706)

The stations differ in altitude and surrounding vegetation as well as in the influence of cold air. The three stations are described in more detail hereafter.

EBG Site

The lowest measuring station is located in the south of Bayreuth in the Ecological Botanical Garden (EBG) of the University of Bayreuth. The measuring station is a 17 m high tower, the base of which is at an elevation of 365 m above sea level. It can be regarded as a rural station since the nearby city has no influence on the air temperature at this station. On a large scale, there can occur a cold-air inflow in case of south winds (in the south of the station there is mainly open grassland with few buildings). The local cold air drainage occurs east-west due to the very gentle slope with the lowest point at the lake (Lüers et al., 2014).

The air temperature is measured with the HMP45 at a height of 2 m, passively ventilated and protected from direct solar radiation and precipitation. In addition, air temperature and humidity are measured with a Frankenberger Psychrometer (due to active ventilation much more accurate values), of which only the dry air temperature values are

used.

Wind velocity and wind direction are measured at an unusual height of 17 m (according to the German meteorological service 10m are the usual height), in order to minimize the disturbing influence of the surrounding trees. The four components of the radiation balance are measured in W/m^2 and comprise global radiation (short-wave incoming radiation), reflected radiation (short-wave outgoing radiation, both measured with the Pyranometer), long-wave outgoing radiation and long-wave incoming radiation of the atmosphere (both measured with the Pyrgeometer).

Other components are also measured at the measuring station in the EBG, but are not mentioned here as they have no direct influence on the occurrence of frost days. The start of the measuring period is the 08th May 1997 for the 2 m height HMP45 measurement, the 15th February 2001 for the 2 m height Psychrometer measurement and the 5 cm height daily minimum measurement.

Voitsumra site

The measuring station at medium altitude is the station near Voitsumra. It is an automatic meteorological station. Like the station in the EBG, it is surrounded by grassland but at an altitude of 624 m above sea level. Voitsumra is located at the edge of the "Weißenstädter Basin", a basin surrounded by several mountains with a height between 780 and 880 m above sea level. In the east, the basin is open, with no surrounding hills (Loos, 2016). As at the EBG, the basic meteorological parameters are measured routinely: Air temperature 2 m above ground (HMP45), wind velocity and wind direction 2 m above ground and the four components of the radiation balance. Due to the valley location of this station, there occurs an accumulation of cold air in cloudless nights. The effects of cold air on the air temperature, especially the minimum temperature, are large at this location. Due to the influence of cold air, this site is therefore a weak wind site at night, but the wind velocities during the day are higher (mostly in an east-west direction) (Loos, 2016). The start of the measurement period is the 30th April 1998 for the 2 m height HMP45 measurement.

Waldstein site

The highest of the measuring stations is the Waldstein site. It is split into two measuring stations, the Waldstein measuring tower in a spruce coniferous forest and the Waldstein container at a clearing near the coniferous forest.

The measuring tower is 32 m high and the base is at an altitude of 775 m above sea level. It is located in a coniferous forest in the north of the Fichtelgebirge. Due to the height of the measuring tower, the air temperature and other meteorological parameters can be measured at different heights and a vertical temperature profile can be created. The start of the measurement period is the 25th November 1998 for the HMP45 measurement

at 2 m height. The measuring container is around 150 m away from the measuring tower and is located in a clearing (distance to the trees approximately 40 m). It is located 10 m lower than the measuring tower, at an elevation of 765 m above sea level. The basic meteorological measurements (air temperature at 2 m height, wind velocity and direction, radiation balance, etc.) as well as special measurements of air pollutants are available since 1994 (Foken et al., 2017). The start of the measurement period is the 24th January 1994 for the 2 m height HMP45 measurement.

There was no phenological data measured at the three meteorological measuring stations. Therefore, phenological data collected and provided by the German meteorological service from two stations nearest to the meteorological stations was used. These stations were Aichig for the EBG (in 2.3 km distance) and Weißenstadt for Voitsumra and Waldstein (in 2.2 km and 5 km distance). From these stations, the phenological data provided by the German meteorological service, climate data center (DWD Climate Data Center (CDC), 2019a,b) was used.

From those, data sets with phenological spring events of grassland (Dauergrünland) with the phenological spring event 'greening begin', coltsfoot (Hufflattich) with 'blooming begin', copper beech (Rotbuche) with 'leaf unfolding begin' and mountain ash (Eberesche) with 'bud break begin', 'leaf unfolding begin' and 'blooming begin' were used. For the mountain ash and the copper beech, phenological fall events were also measured and available. These were used to calculate the phenological vegetation period (see in section 3.4.2).

The German and Bavarian average of frost days and ice days was provided by the German meteorological service, climate data center (2019), as well.

2.2 Measuring Instruments

At the stations, the parameters are recorded as 10 minute averages by a data logger. At all stations, the temperatures are measured with a Vaisala HMP45 temperature sensor. The measurement is made by a platinum resistance thermometer (Pt-100) and has an accuracy of $\pm 0.2\text{K}$ at 20°C . But since this Pt-100 is only protected from radiation by a weather hut, the measurement inaccuracy can rise to 1K as the hut is heating up (Foken, 2017).

At the EBG and the Waldstein Tower, the temperatures are also measured with a Frankenberger Psychrometer, which is ventilated and protected from radiation to exclude the influence of wind and radiation on the temperature measurement as far as possible. The measurement is made with platinum measuring resistors (Pt-100) and has a measurement uncertainty of $\pm 0.1\text{K}$ at 0°C .

2.3 Data Analysis with R

The data analysis is done with R (version 3.4.2), a free software of the R Foundation for Statistical Computing. The meteorological data is available at the BayEOS Server and can be loaded in R via the BayEOS-Package. The time series are archived as zoo series (using the zoo-package) and can be used for further statistical data analysis. The phenological data is available on the German meteorological service Climate Data Center Server.

As the data is provided as 10-minute mean temperature, the data has been aggregated to a daily level to obtain the mean daily temperature, the minimum daily temperature and the maximum daily temperature.

With the daily minimum temperature, specific winter indices such as the number of frost days, the absolute minimum temperature, the first and last frost day and the frost-free period were calculated. The mean frost period temperature was calculated with the daily mean temperature for the frost-influenced time (period start is the mean first frost day and period end is the mean last frost day of the respective station). Additionally, continuous frost days were subsumed to frost events and continuous ice days were subsumed to ice events. Then, event based indices like the number of frost (ice) events and the mean frost (ice) event length were calculated.

A threshold of 0°C was used to calculate the frost days ($T_{\min} < 0^{\circ}\text{C}$) and ice days ($T_{\max} < 0^{\circ}\text{C}$) as this is the most commonly used threshold for these calculations. This threshold is mentioned in the weather encyclopedia of the German meteorological Service (2019) and in most literature such as Frich et al. (2002); Kiktev et al. (2003); Bonsal et al. (2001); Klein Tank and Können (2003). However, in some cases, different thresholds were used, such as -2.2°C (Schwartz et al., 2006), -2°C (Rochette et al., 2004) and -1°C (Scheifinger et al., 2003).

In order to obtain a valuable statistical annual analysis, the frost indices were aggregated per winter year (def. winter year 2018: Day of the Year 198 2017 to Day of the Year 197 2018). A summary of the calculated frost indices is given in table 1.

To determine possible correlations between winter indices, a correlation analysis was done for the number of frost days with the mean frost period temperature (see in section 3.2.5). A correlation analysis was also performed for the number of frost and ice days of each meteorological station with the Bavarian average to determine whether the station is mainly dependent on the general weather situation or influenced by local microclimatic conditions (see in section 3.2.2).

These correlation analyses were visualized using scatter plots and quantified with the Pearson Product-Moment Correlation test.

The Mann-Kendall trend test was used to identify possible trends in the indices over time. This test is mainly used to analyze data for continuously increasing or decreasing

trends. It is a non-parametric test (i.e. the data does not have to follow a normal distribution). The test is applicable to few data points, but the more data points available, the greater the probability of finding a true trend, as opposed to a random trend (McLeod, 2011). The Mann-Kendall trend test was used only to calculate the p-value of a possible occurring trend. If the p-value was below 0.2, the trend rate was calculated using a linear regression model.

Table 1: Summary of the climatological frost indices, their calculation and unit

Climatological Frost Indices	Calculation	Unit
Mean Frost Period Temperature	average of the daily mean temperature between the mean first and mean last frost day	°C
Number of Frost Days	sum of days with daily minimum temperature below 0°C	Days per Winter Year
Number of Ice Days	sum of days with daily maximum temperature below 0°C	Days per Winter Year
Minimum Temperature	minimum of the daily minimum temperature per winter year	°C
Date of the Minimum Temperature	date of the minimum of the daily minimum temperature per winter year	Date
First Frost Day	first day of the winter year with the daily minimum temperature below 0°C	Date
Last Frost Day	last day of the winter year with the daily minimum temperature below 0°C	Date
Frost-free Period	number of days between the last frost day and the subsequent first frost day	Days per Calendar Year
Number of Ice Events	number of consecutive ice days (summarized as an ice event)	Number per Winter Year
Mean Ice Event length	mean number of consecutive ice days per ice event	Days per Winter Year
Maximum continuous ice event	maximum of consecutive ice days per winter year	Days per Winter Year

2.4 Pre-Analysis: Data Gaps

In general, the Psychrometer temperature data is more accurate compared to the HMP45 temperature data. However, the measuring period of the Psychrometer measurement was shorter (first usable winter year 2002, measurement at the EBG) and there were no Psychrometer measurements at the Voitsumra site and at the Waldstein Container (as opposed to HMP45 measurements). Thus, the HMP45 measurements were used for data analysis in order to analyze the longest time period and to ensure the best comparability between the measuring points.

Since the measurements started at different times, the first usable winter year is 1998 (2m height, HMP45) or 2002 (5cm height, daily minimum) in the EBG, 2000 at Voitsumra (2m height, HMP45), 1995 at Waldstein Container (2m height, HMP45) and 2000 at Waldstein Tower, depending on measuring station and measuring instrument.

Unfortunately, there are several data gaps, thus not every winter year of the time series can be used. Therefore, the winter years 2015 and 2016 for the EBG HMP45 measurement (2m height), the winter years 2000, 2003, 2007-2009, 2012 and 2013 for the Voitsumra HMP45 measurement and the winter years 2006, 2008 and 2014 for the Waldstein Container HMP45 measurement should have been excluded from the calculations. To examine the possibility to fill the data gaps with other temperature data, the in the following described analysis was done.

Figure 7 shows Hovmöller plots of the daily temperature data in which the missing data for all three stations can be seen for comparison.

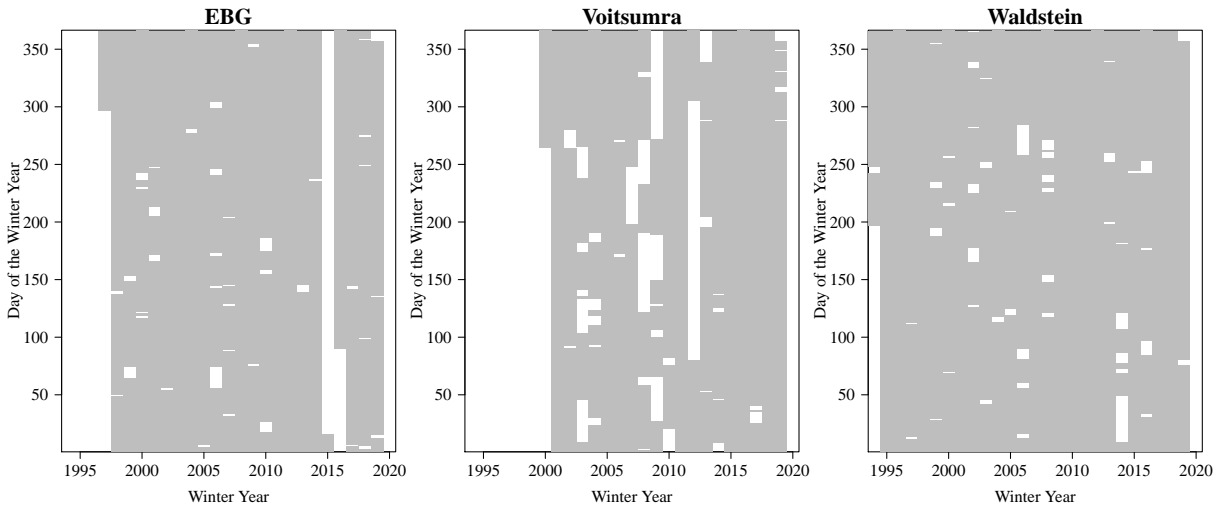


Figure 7: Hovmöller plots of the daily 2m height HMP45 temperature data at the EBG, Voitsumra and Waldstein. Days with valuable data are shown in grey, days with more than 10% missing data are shown in white. At the EBG a large data gap occurs in winter year 2015 and 2016, the most data gaps occur at the Voitsumra site.

Since 15th February 2001, the air temperature was also measured at a height of 2m using a Frankenberger Psychrometer at the EBG station. Therefore, the data gap around the winter years 2015 and 2016 of the HMP45 measurements could be filled with the Psychrometer data. In order to determine the consistency of these two measurements, the temperature data measured with the HMP45 was compared with the temperature data measured with the Psychrometer in the following.

In general, the Psychrometer measurements are more exact due to the active ventilation (see in section 2.2). As the HMP45 is only passive ventilated, it overestimates temperature at day, but underestimates at night. This can be clearly seen in figure 8.

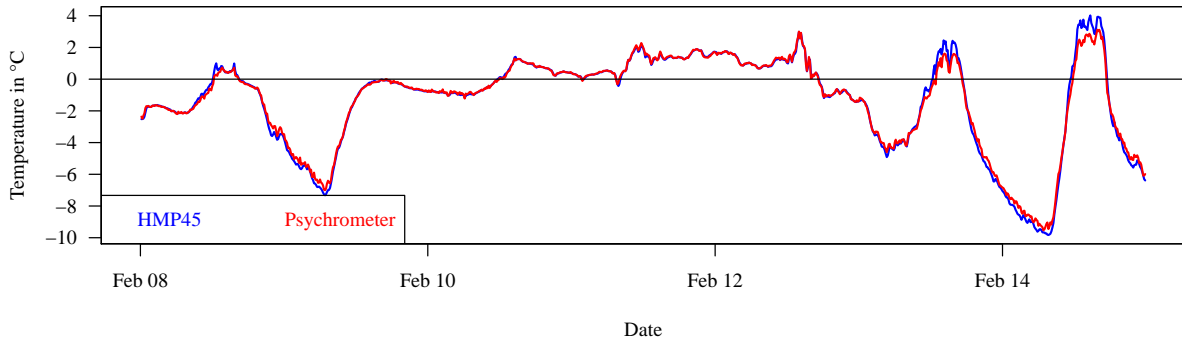


Figure 8: Temperature measured at 2m height in February 2018 with the HMP45 (blue) and the Psychrometer (red) at the EBG station

To visualize the difference between these two measurements over the entire measurement period, the daily mean, minimum and maximum temperatures measured with the HMP45 versus the daily mean, minimum and maximum temperatures measured with the Psychrometer are shown in figure 9 along with a red line of equality.

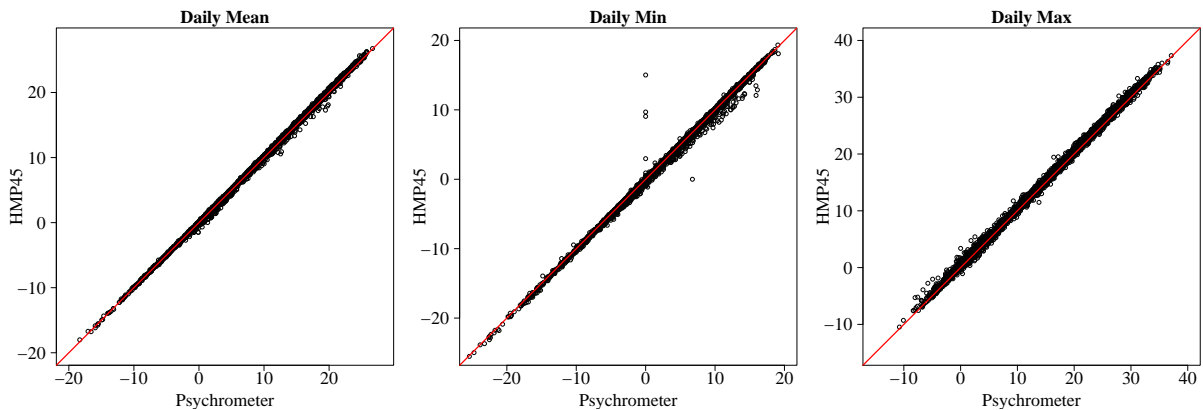


Figure 9: Scatterplot of the aggregated mean, minimum and maximum temperature data measured with the HMP45 against measured with the Psychrometer at the EBG station. A line of equality ($x=y$ line) is shown additionally.

It becomes visible that the temperature values for the daily mean are indeed well correlated. This correlation was confirmed using the Pearson correlation test (correlation coefficient of 0.99 and a $p < 0.001$). But since the temperature is overestimated during the day and underestimated at night, the mean value of the 24 h is more accurate and comparable with the daily mean of the Psychrometer. The differences should be greater for the daily minimum and maximum temperatures. Therefore, the daily minimum temperature and the daily maximum temperature measured with the HMP45 were plotted versus the respective temperature measured with the Psychrometer. In fact, the measurements for the daily minimum temperature fit together better at low temperatures (below 0°C) than at higher temperatures, while the measurements for the daily maximum temperature fit together better at higher temperatures. Overall, one can see that the outliers are larger,

but overall they are still well correlated.

Figure 10 shows the mean frost period temperature of the HMP45 measurement versus the Psychrometer measurement. The mean frost period temperature was calculated as the winter year average of the daily mean temperature between the mean first and the mean last frost day respectively.

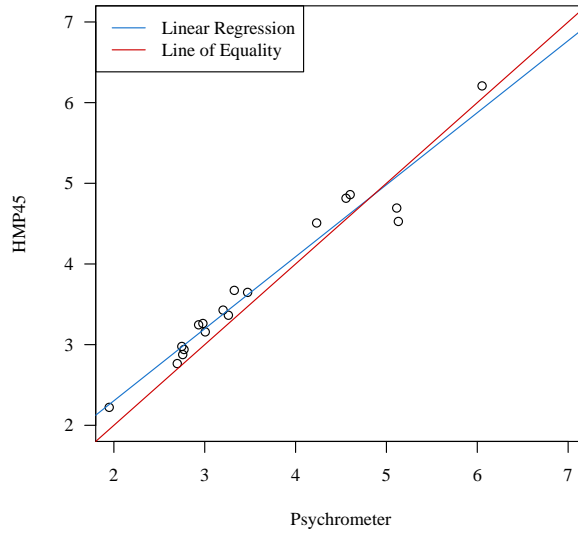


Figure 10: Scatterplot of the mean frost period temperature measured with the HMP45 versus measured with the Psychrometer, EBG. A linear regression line is plotted in blue, a line of equality ($x=y$ line) in red.

The values seem to be better correlated at lower mean frost period temperatures than at higher temperatures. Nevertheless, the Pearson correlation test showed a high correlation with a correlation coefficient of 0.98 and a $p < 0.001$ (highly significant). Linear regression was calculated for the two measurements, shown in figure 10 as a blue line (linear equation: $y = 0.52 + 0.89 \cdot x$). Since the linear model has a gradient of almost 1, the measurements are very similar.

The mean frost period temperature was calculated with the daily mean temperature, which should be better correlated than the daily minimum and maximum temperature. In order to compare a parameter calculated with the daily minimum temperature, the number of frost days, calculated with the HMP measurement and the Psychrometer measurement, is compared in a scatter plot in figure 11.

Although there are some outliers, the number of frost days measured with the HMP45 or the Psychrometer is similar in most winter years. Since the daily minimum temperature is used to calculate the frost days and the daily minimum is often underestimated in the HMP45 measurement, the differences between the measurements are larger. More frost days are measured with the HMP45 and thus the linear regression line has a gradient not equal to 1 (linear equation: $y = 9.14 + 0.93 \cdot x$). The correlation was validated by the Pearson correlation test, which found a correlation coefficient of 0.95 and a $p < 0.001$.

This result corresponds to the expectations of a lower correlation coefficient and a worse p-value than for the correlation of the mean frost period temperature.

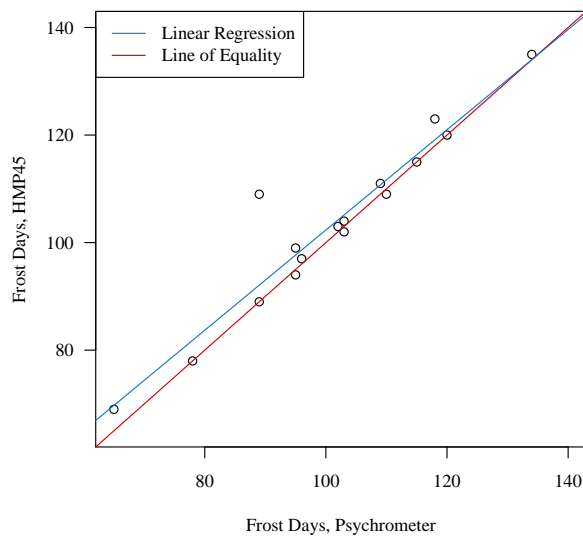


Figure 11: Scatterplot of the number of frost days measured with the HMP45 versus measured with the Psychrometer, EBG. A linear regression line is plotted in blue, a line of equality ($x=y$ line) in red.

Since the daily temperature data and the calculated data fit well, the data gap in the winter years 2015 and 2016 in the HMP45 measurement was filled with the Psychrometer Data.

In order to obtain a longer time series for the EBG measurement at 2 m height, the time before the measurement starts at the EBG station (08th May 1997) was filled with adjusted data from the former EBG station. This station was positioned 500 m in western direction from the current station. If data gaps occurred in this time series, they were filled with temperature data from the Heinersreuth station, maintained by the German meteorological service.

For the Voitsumra station, several large data gaps were detected, as well. For this station, it is a bit more difficult to fill the gaps because this location is strongly influenced by cold air drainage / pooling. Nevertheless, the data gaps were filled with adjusted data from the station Fichtelberg – Hüttstadel (maintained by the German meteorological service). The calculations of the climatological frost indices were done with these filled data sets for the EBG and the Voitsumra stations.

3 Results

In the following sections the results are first shown and described for the EBG. In the EBG two measurements were performed at two heights. Therefore, the results of these two measurements are initially shown alone. Then the results of the different stations are compared.

3.1 Annual Course and Distribution of the Daily Temperature

In order to get an overview of the daily temperature data and the distribution of frost days, the daily minimum temperature data is illustrated in a Hovmöller plot. For this representation the daily minimum temperatures are arranged as matrix and each day is assigned to a certain color.

In the following, a Hovmöller plot of the filled daily minimum temperature data measured at 2m height, mainly with a HMP45 at the EBG is shown. The black lines show the calculated mean start and end of the frost-influenced period (as described in section 2.3).

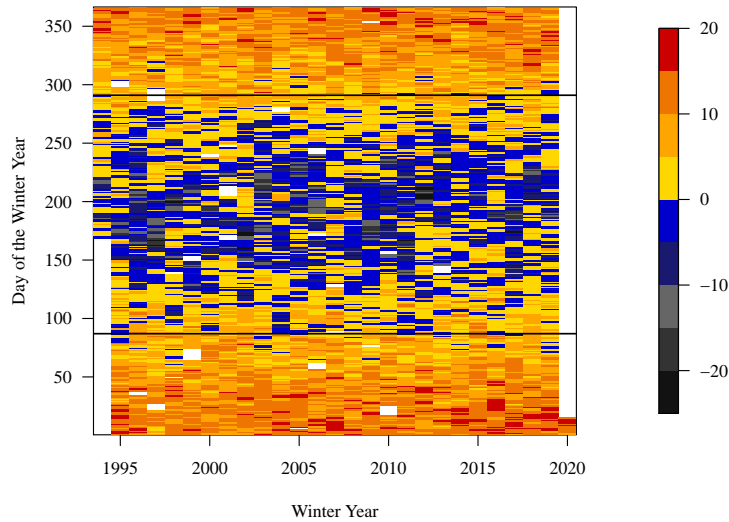


Figure 12: Hovmöller plot of the daily minimum temperature data, EBG. All frost days (T_{\min} below 0°C) are depicted in blue. The mean first and last frost days are shown with two black lines. Data gaps are shown in white.

The daily minimum temperature ranges from -25°C to 20°C , as one can see in the legend in figure 12. All frost days (T_{\min} below 0°C) are depicted in blue. Thus, the distribution and frequency of frost days becomes visible. For example, in the winter year 2007 notably few frost days occur (similar at the Voitsumra and the Waldstein site).

The mean start and end of the frost-influenced period are also shown as black lines to give a rough idea about the mean frost period length. At the EBG site, the mean start of the mean frost period is the 11th October and the mean end of the mean frost period is

the 3rd May. The period in between is called the mean frost period and is described more detailed in section 3.2.1.

The same analysis was done for the Voitsumra and the Waldstein site, see figure 57 (Voitsumra) and figure 58 (Waldstein Container) in the Appendix.

The daily aggregated temperatures of the EBG, Voitsumra and the Waldstein are also shown in the Appendix in figure 53 (EBG), figure 54 (Voitsumra), figure 55 (Waldstein Container) and figure 56 (Waldstein Tower).

The change in the minimum and maximum temperatures at the EBG site is shown in two histograms in figure 13. In the Histograms, the distribution of daily temperatures is illustrated for two periods, the first from 1999 to 2008 and the second from 2009 to 2018.

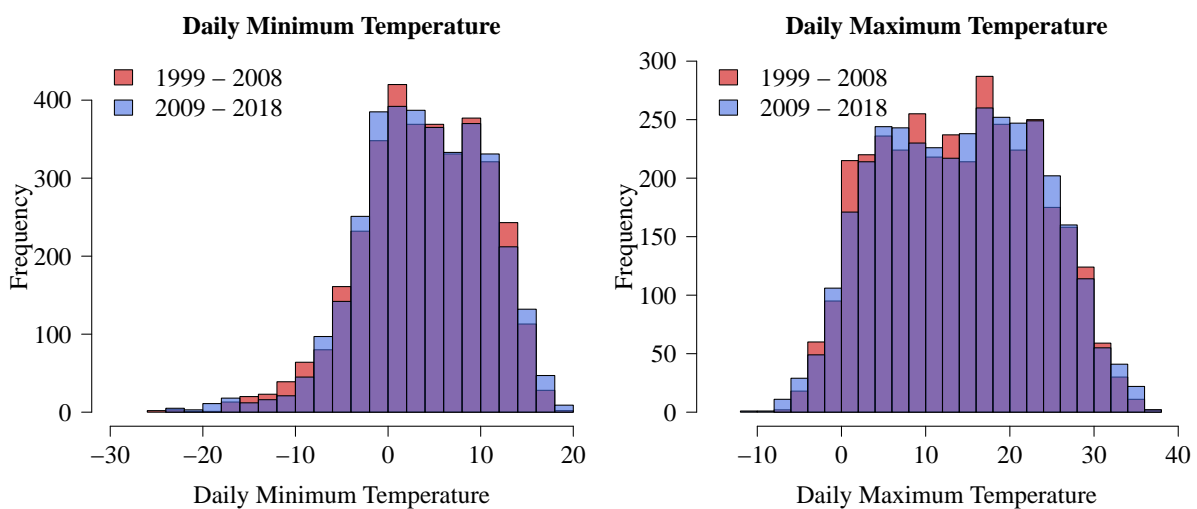


Figure 13: Histograms of the daily minimum and the daily maximum temperature at the EBG site, for the period 1999 – 2008 (red) and the period 2009 - 2018 (blue)

The change in the daily minimum temperatures is showing a various pattern and no uniform trend (e.g. towards higher minimum temperatures). Nevertheless, a trend towards a higher variance occurs. More specified, in the second period more maximum temperatures occur (in the daily minimum and maximum temperature) with at least same often occurring minimum temperatures. The temperatures slightly below 0°C occur for example more often in the second period, while temperatures between -8°C and -16°C occur less often in the second period. In the lowest daily minimum temperatures, an increase in the frequency appears for the second period.

For the daily maximum temperatures, the change is showing a similar various pattern. For the temperatures around 0°C a slight trend to a lower frequency appears. But the lowest daily maximum temperatures occur more often in the second period. Nevertheless, a trend seems to appear towards a higher variance.

The daily minimum and maximum temperatures at the Voitsumra site are as well shown in a histogram in figure 14. The frequencies of the daily temperatures are plotted for the same periods as at the EBG site (1999 - 2008 and 2009 - 2018). In the histograms,

3. RESULTS

no uniform trend appears. In the daily minimum temperatures, the frequencies appear to increase and decrease haphazardly.

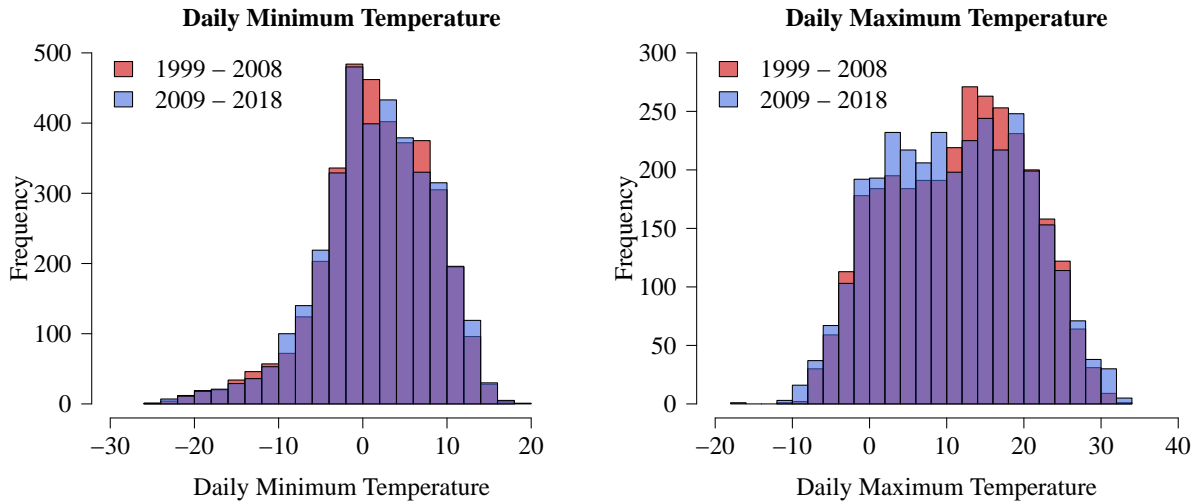


Figure 14: Histograms of the daily minimum and the daily maximum temperature at the Voitsumra site, for the period 1999 – 2008 (red) and the period 2009 - 2018 (blue)

In the daily maximum temperatures, the frequency of temperatures between -2°C and 10°C are increased in the second period. The temperatures between 10°C and 18°C occur, though, less often in the second period.

The histograms of the daily minimum and maximum temperatures are shown for the Waldstein site in figure 15. The frequencies of the daily temperatures are shown for two periods, the first from 1999 to 2008 and the second from 2009 to 2018.

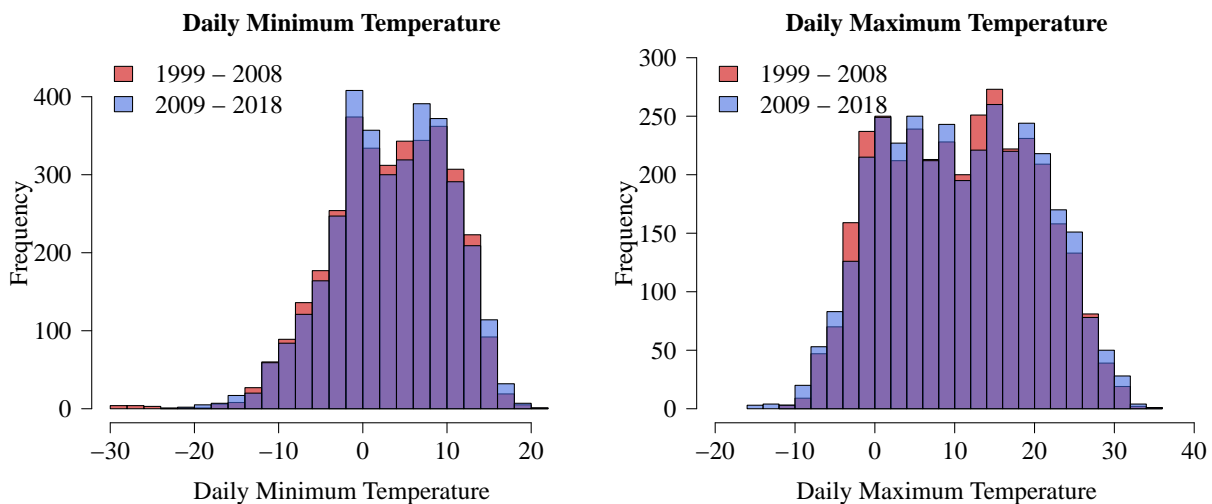


Figure 15: Histograms of the daily minimum and the daily maximum temperature at the Waldstein site, for the period 1999 - 2008 (red) and the period 2009 - 2018 (blue)

At this site, the minimum temperatures around 0°C occur more frequently in the second period. The frequency of minimum temperatures below -2°C are decreasing all in all.

The daily maximum temperatures between -4°C and 0°C occur less often in the second period, while temperatures lower than -4°C occur more often in the second period. The frequencies of the daily maximum temperatures above 0°C are decreasing and increasing haphazardly.

3.2 Winter Indices

In the following, the course of the annual average of the climatological frost indices is shown per winter year. For the most sections, the results are shown first for the EBG and then compared between the three stations. Temperature indices such as the mean frost period temperature and the coldest day are presented first. Frost indices like the number of frost days per winter year are displayed after. Finally, in the last section, there are described several comparisons between indices.

3.2.1 Mean Frost Period Temperature and Coldest Day

Mean Frost Period Temperature

The mean frost period temperature was calculated as the mean temperature between the mean first and mean last frost day of the respective measuring station (for Voitsumra and EBG with the filled data sets). In this section, the results are depicted directly as comparison between the stations.

In coincidence with the general rise of the global temperature and as the temperature in winter and spring is likely to rise more than in other seasons (for example Sparks and Menzel, 2002) one would expect that this change in temperatures is reflected in the calculated mean frost period temperature.

The mean frost period temperature of the three measuring sites is shown in figure 16.

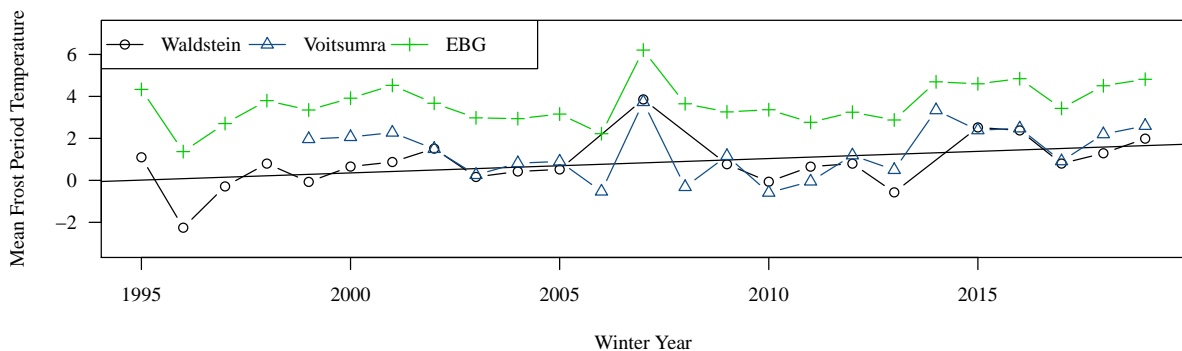


Figure 16: Comparison of the mean frost period temperature between the three station. The Waldstein station is shown in black, the Voitsumra station in blue and the EBG station in green. A linear regression line is depicted for the Waldstein results, as there occurs a significant trend.

The mean winter temperature is always highest at the EBG site. The course of the

mean winter temperature is often similar at the EBG and Waldstein sites, whereas the temporal evolution at the Voitsumra site seems to be rather decoupled.

In general, there was no trend detected at the Voitsumra site. However, at the Waldstein Container site, there seems to be a slight trend to higher mean frost period temperatures. According to the Mann-Kendall trend test, there is a significant positive trend to higher mean frost period temperatures with a rate of 0.068 and $p = 0.055$. For the EBG site, there was a non-significant positive trend discovered (rate of 0.048, $p = 0.14$).

Coldest Day in the EBG

The temperature is rising, especially in winter and spring (Bonsal et al., 2001; Sparks and Menzel, 2002; Robeson, 2004). Thus, this effect was also expected to be reflected in the minimum temperature per winter year as underlying basis of the here described analysis.

In figure 17 the minimum temperature per winter year is pictured at the EBG measuring station.

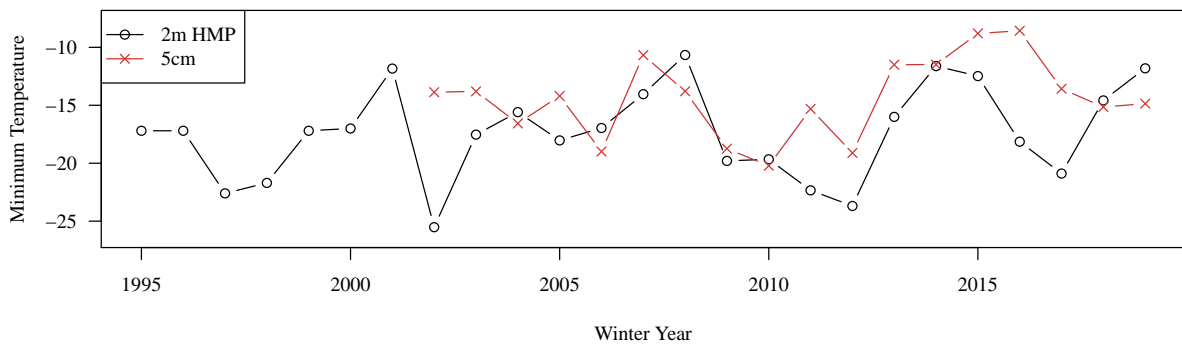


Figure 17: Minimum temperature per winter year at the EBG site. The minimum temperature at 2 m height is shown in black, at 5 cm height in red.

The minimum temperature per winter year ranges between -25.52°C and -10.66°C (HMP45 at 2 m height), or between -20.22°C and -8.57°C (Daily Minimum at 5 cm height). In general, the minimum temperatures are lower at the 2 m height measurement.

In some winter years the minimum temperature differs very much at the two different measuring heights. This is mostly driven by the fact, that in the most years, the minimum temperature at the two heights is measured on different days in the winter (see in figure 18). If the date of the minimum temperature coincide for the both heights (for example winter year 2014), the minimum temperature is very similar as well. The minimum temperature per winter year is variable over the measuring period. No trend was found with the Mann-Kendall trend test.

There can be very different dynamics, which can cause the measurement of the minimum temperature at the two different measurement heights. At 2 m height, the coldest events often takes place with snow coverage (then, the instrument at 5 cm height is likely to be covered and to measure temperatures just a bit below 0°C).

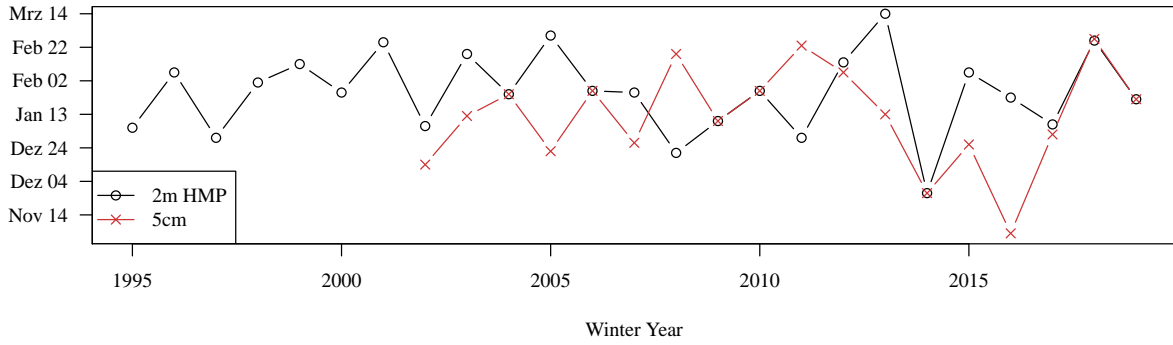


Figure 18: Date of the minimum temperature per winter year in the EBG. For the 2 m height measurement shown in black, for the 5 cm height in red.

Another possibility to measure very cold events is, if the wind comes from East/North East and brings very cold air from Siberia. Then, very cold temperatures are measured at both heights (2 m and 5 cm).

Comparison of the three different measuring stations

In the following, the minimum winter temperature is compared between the three different sites. In figure 19 the minimum winter temperature at the three sites is illustrated.

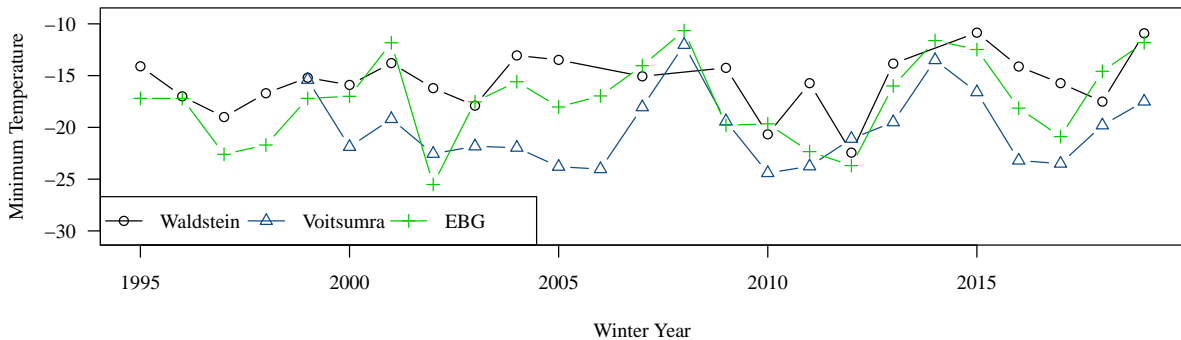


Figure 19: Comparison of the minimum temperature per winter at the three stations. The Waldstein station is shown in black, the Voitsumra station in blue and the EBG station in green.

The minimum temperature at the Waldstein and the EBG site is positive correlated, with a correlation coefficient of 0.63 and $p = 0.002$. For the Voitsumra and the EBG site, a positive correlation with a correlation coefficient of 0.69 and $p < 0.001$ was discovered. On the contrary, between the minimum temperatures of the Voitsumra site and the Waldstein site, no significant correlation occurs. The lowest minimum temperatures occur at the Voitsumra site (average of -20°C) while the highest minimum temperature mostly occurs at the Waldstein site (average of -16°C).

In general, there does not seem to be any trend towards lower or higher minimum winter temperatures. Supporting this, no significant trends were detected with the Mann-

Kendall trend test.

In figure 20 the date of the minimum winter temperature at the three sites over a course of 24 years (20 years) is depicted.

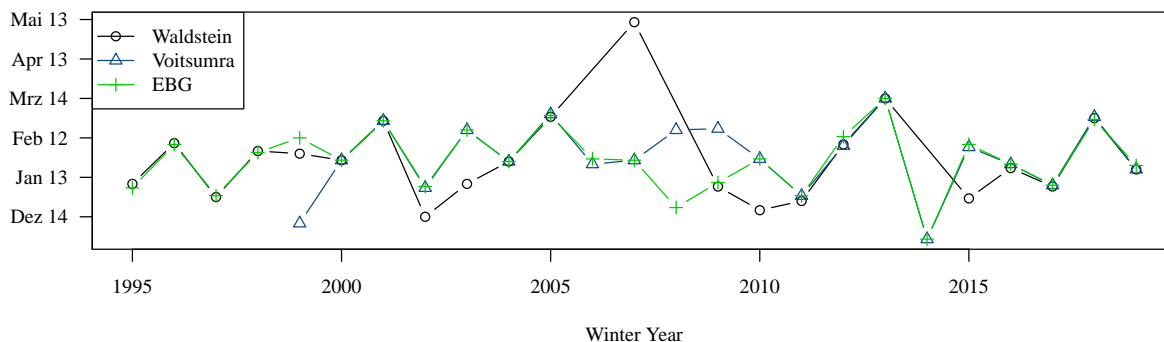


Figure 20: Comparison of the date of the minimum temperature per winter at the three stations. The Waldstein station is shown in black, the Voitsumra station in blue and the EBG station in green.

It appears that the day of the minimum temperature often falls together at the three sites. This could explain the similar course of the minimum temperature in figure 19.

3.2.2 Frost and Ice Days

Results of the EBG

In the following, the absolute number of frost and ice days per winter year at the EBG is shown and described.

In figure 21, the absolute number of days per winter with a minimum temperature below 0°C are compared with the absolute number of days with maximum temperature below 0°C, thus, the number of frost days with the number of ice days.

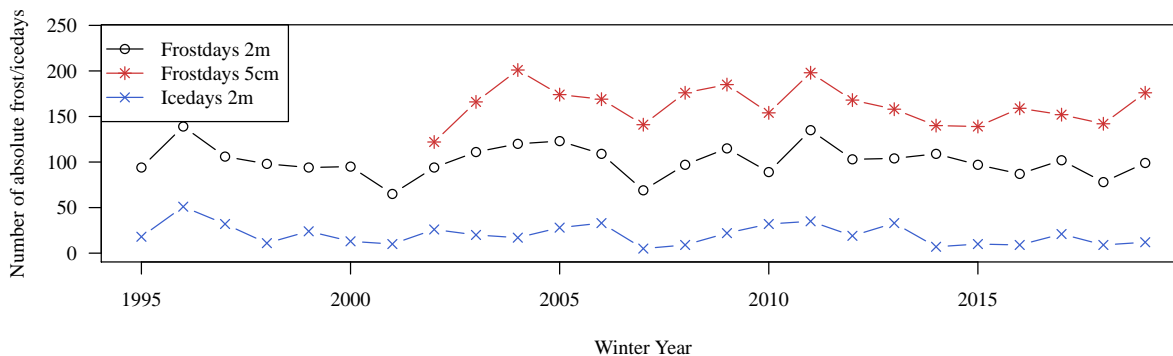


Figure 21: Absolute number of ice and frost days per winter, EBG. The frost days at 2 m height are shown in black, those at 5 cm height are shown in red. The ice days are depicted in blue.

For the calculation of the ice days, only the measurements at 2 m height were used. The measuring instrument at 5 cm height is measuring the daily minimum, whereas, for

calculating the ice days, the daily maximum is used. Thus, only ice days and events at 2 m heights were considered.

The difference between the 2m measurements and the 5cm measurements is large. But the temporal evolution is often highly correlated (correlation coefficient of 0.69, $p = 0.0014$).

Moreover, the number of ice days per winter is much lower than the number of frost days. The mean number of frost days is 101, while the mean number of ice days is 20 (across the measuring period). This matches the expectation because in our latitudes days during which the minimum temperature drops below 0°C occur much more often than days during which the maximum temperature is constantly below 0°C . One should also have in mind that the absolute number of frost days include the absolute number of ice days (as an ice day is a frost day, too).

There is no detectable significant trend in the frost days. It is possible that the former ice days develop to frost days and that therefore the absolute number of frost days per winter does not decline. However, in the mean number of frost and ice days of Bavaria and Germany do not support this hypothesis, as the frost days are decreasing with a higher rate than the ice days. At the EBG station neither the number of frost days nor the number of ice days decline. This was expected, if the global warming trend shows in the local climate and as the decline of the number of frost days is found in the literature. However, the time series might be too short to enable the detection of a trend. Furthermore, as in the case of the average number of frost and ice days of Bavaria and Germany the trend could have already occurred before 2000.

Comparison of the three different measuring stations

In figure 22, the absolute number of frost days per winter year is displayed for the three different sites along with the average number of frost days of Bavaria.

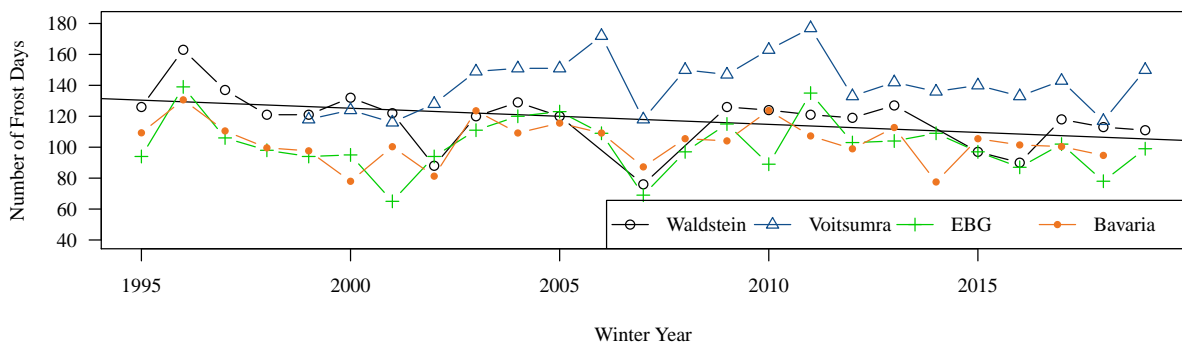


Figure 22: Comparison of the number of frost days between the different stations. The Waldstein station is shown in black, the Voitsumra station in blue and the EBG station in green. The Bavarian average of frost days is pictured additionally in orange. A linear regression line is shown for the Waldstein site, where the number of frost days is decreasing.

The most frost days occur at the Voitsumra site with an average of 141 frost days. The number of frost days is mostly similar at the Waldstein and the EBG site (17 days difference of the averages). The two sites are well correlated as well, with a correlation coefficient of 0.58 and $p = 0.005$.

While the number of frost days seems to stagnate during the measuring period at the EBG and at the Voitsumra site (no trends were detected with the Mann-Kendall trend test), a slight decrease was observed at the Waldstein site from 126 frost days in winter year 1995 to 111 frost days in winter year 2019. A significant negative trend with a rate of -1.0 and $p = 0.0051$ was observed using the Mann-Kendall trend test. Thus, at the Waldstein site, there occur around 10 less frost days per decade.

The number of frost days seems similar with the Bavarian average for the EBG and the Waldstein site. The Voitsumra site, though, appears to be decoupled (always higher, but the temporal evolution is sometimes similar). The correlation between the stations and the Bavarian average is described in more detail in section 3.2.5.

In figure 23 the absolute number of ice days at the three different sites is shown.

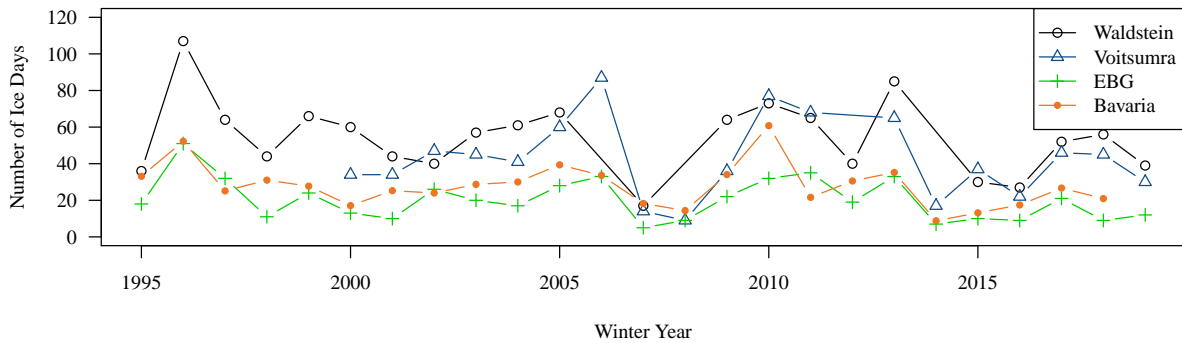


Figure 23: Comparison of the number of ice days between the different stations. The Waldstein station is shown in black, the Voitsumra station in blue and the EBG station in green. The Bavarian average of ice days is pictured additionally in orange.

The number of ice days is nearly always lowest at the EBG site, with an average of 20 days. But it does not differ so clearly between the Waldstein and Voitsumra sites as it does for frost days. The two stations are highly correlated with a correlation coefficient of 0.78 and $p < 0.001$. The order of the stations is not that clear, like at the frost day calculations, probably because the daily maximum temperature is mostly measured during the day, when the Voitsumra site is not cold-air influenced.

At the EBG, the number of ice days seems to stagnate during the measuring period, while it seems to decline at the Waldstein site and maybe also at the Voitsumra site. However, examined with the Mann-Kendall trend test, no significant trend appears at any of the sites.

At the Waldstein and the Voitsumra site, the number of ice days is nearly always higher as the Bavarian average. In contrary, the Waldstein site was similar to the Bavarian

average for the frost days. However, for the ice days, the Bavarian average is similar to the EBG site. The correlation between the stations and the Bavarian average is described and illustrated more detailed in section 3.2.5.

3.2.3 First and Last Frost Day

Results of the EBG

According to Schwartz et al. (2006), the length of the frost period is decreasing, caused by later occurring first frost days in autumn and primarily driven by earlier last frost days in spring.

To review if this trend also appears in our local and temporal context, the date of the first and the last frost day is depicted for the EBG station (figure 24).

The first frost day in autumn mostly occurs earlier at 5 cm height than at 2 m height. However, for instance in 2009, the frost day was recorded at the same day. In the winter year 2019, the first frost day is very early at the 5 cm height (August 2018). Checked with the Mann-Kendall trend test, there is no trend at the 2 m height HMP45 measurement.

At the 5 cm height measurement, the early date of the first frost day in winter year 2019 was scope of further analysis. In figure 25, the temperature of this first frost event is plotted. This first frost event occurred in the night of the 26th August 2018 from 04:40 am to 05:40 am. The next frost event occurred one month later from the 25th September 2018 until the 01st October 2018 with more pronounced temperatures below 0°C. Therefore, it is assumed, that the first frost day on 26th August 2018 has no large impact on plants. For the trend analysis, the second frost event was used.

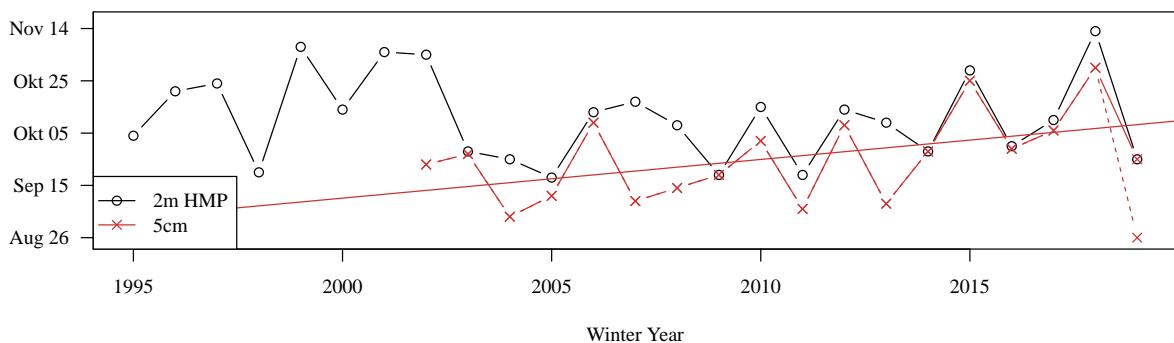


Figure 24: Date of the first frost day at the EBG. The 2 m height measurement is shown in black, the 5 cm height measurement in red. In winter year 2019, two dates are depicted, the one with the dashed line is the original first frost day. A linear regression line is depicted additionally, as there appears a trend in the 5 cm measurements.

If one omits the date of the first frost day in the winter year 2019 at the 5 cm height measurement and replaces it with the date of the second frost day in the winter year 2019, a significant trend towards a later occurring first frost day emerged with a rate of 1.5 and $p = 0.069$.

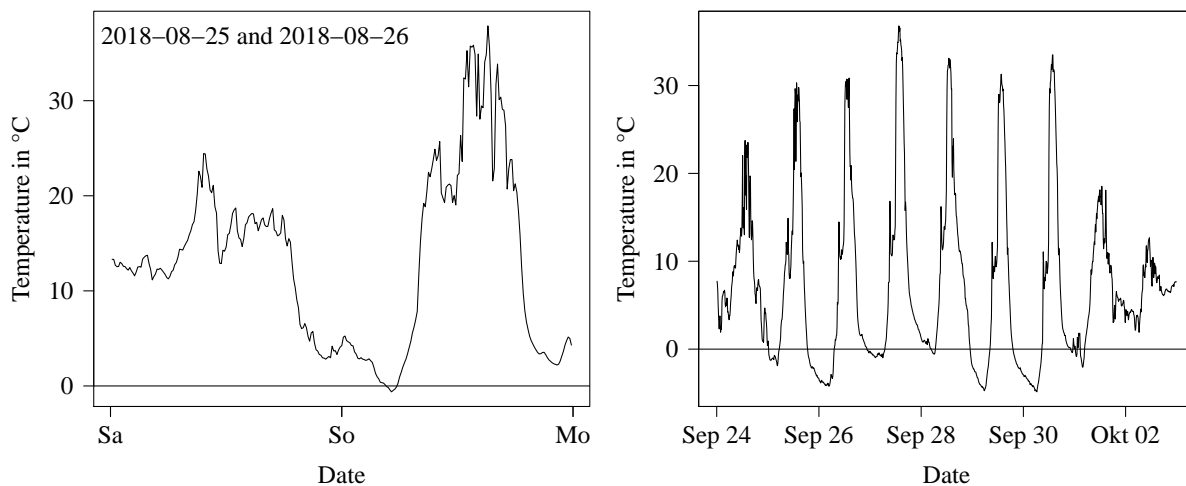


Figure 25: Temperature course at the date of the first and second frost day, winter year 2019, EBG

In figure 26 the date of the last frost event per winter year is pictured for the EBG. Here, the differences between the 2 m measurement and the 5 cm measurement are greater and more distinct. The last frost day is always measured earlier at the 2 m height measurement.

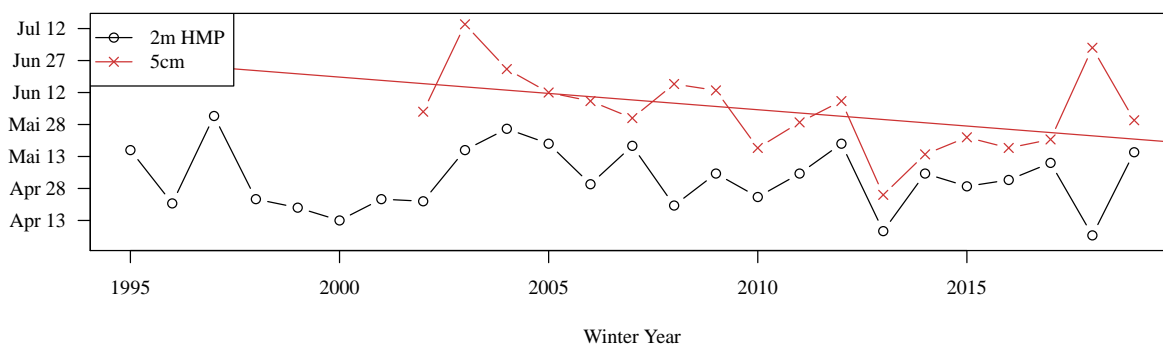


Figure 26: Date of the last frost day at the EBG station. The 2 m height measurement is shown in black, the 5 cm height measurement in red. A linear regression line is depicted additionally, as there appears a trend in the 5 cm measurements.

At the last frost day calculation of the 5 cm height measurement, a negative trend towards earlier last frost days with a rate of -1.5 and $p = 0.049$ was found. Thus, at the 5 cm height measurement the last frost day in spring occurs earlier in the year with a rate of -15 days per decade. However, this trend is not reflected in the last frost day at the 2 m height measurement.

Comparison of the three different measuring stations

In the following, the first frost day and the last frost day are compared between the three measuring stations at the EBG, the Voitsumra and the Waldstein site.

3. RESULTS

The date of the first frost day in autumn is shown for every measuring station in figure 27.

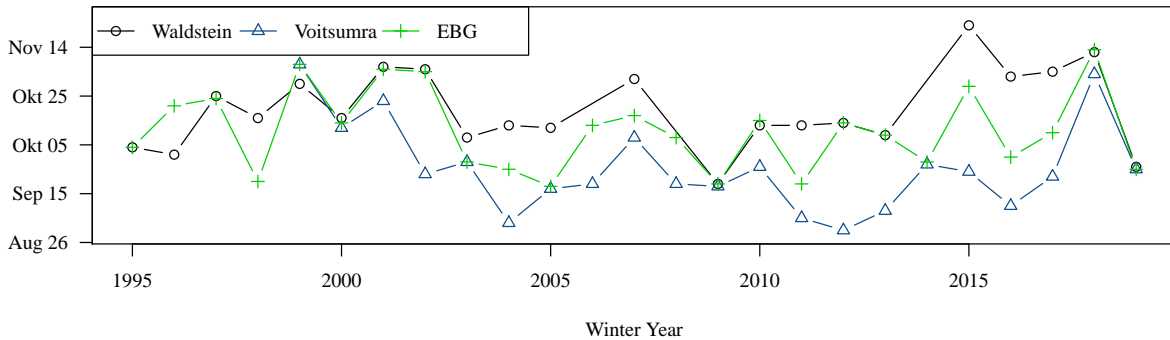


Figure 27: Comparison of the date of the first frost day between the three stations. The Waldstein station is shown in black, the Voitsumra station in blue and the EBG station in green.

The first frost day is often earliest at the Voitsumra site, averaged at the 26th September. At the Waldstein site, the first frost day is generally measured latest, averaged at the 20th October.

Tested with the Mann-Kendall trend test, none of the first frost day calculations is showing a significant trend to later first frost days.

In figure 28 the date of the last frost event in spring is shown for the three measuring stations.

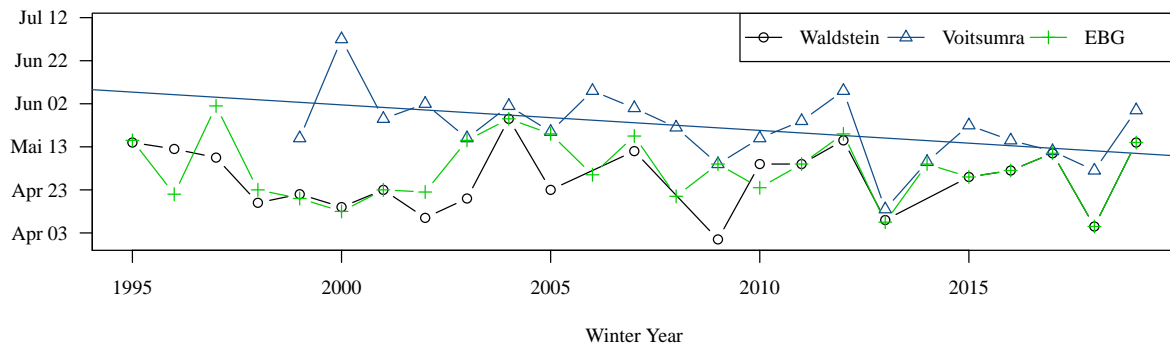


Figure 28: Comparison of the date of the last frost day between the three stations. The Waldstein station is shown in black, the Voitsumra station in blue and the EBG station in green. A linear regression line is shown additionally for the Voitsumra station, as there occurs a significant negative trend.

Comparable to the calculation of the first frost day, the last frost day is mostly latest at the Voitsumra site, averaged at the 22nd May. Thus, at the Voitsumra site there is the longest frost period and the shortest frost-free period (see section 3.2.4). Meanwhile, the last frost day is at nearly similar days at the EBG and the Waldstein site with 5 days difference between the averages.

No significant trend (e.g. towards an earlier last frost day) was detected at the Waldstein site nor the EBG site using the Mann-Kendall trend test. At the Voitsumra measurement, however, there is a negative trend towards earlier last frost days in spring, with a rate of -1.19 and $p = 0.057$.

3.2.4 Frost-free Period

Caused by primarily the trend in the last frost day in spring occurring earlier, the length of the frost-free period is increasing by 4.9 days per decade over the period 1951 - 2000 (Menzel et al., 2003). Based on the dates of the first and last frost day, the frost-free period was calculated. The frost-free period is calculated and plotted per calendar year. Thus, the first shown year is 1994 or 2001 for the 2 m or 5 cm height measurements respectively. The same applies for the Waldstein and the Voitsumra site with the first shown year 1994 or 1999 respectively.

The frost-free period is shorter at the 5 cm height measurement with averaged 112 days, than at the 2 m height measurement with averaged 162 days. This is consistent with the finding that the first frost day occurs averaged 15 days earlier at the 5 cm measurement and the last frost day occurs averaged 32 days later at the 5 cm measurement than at the 2 m measurement. This is lengthening the frost period and shortening the frost-free period at the 5 cm measurement compared to the 2 m measurement (see section 3.2.3).

Results of the EBG

In figure 29 the number of days of the frost-free period is shown for the EBG.

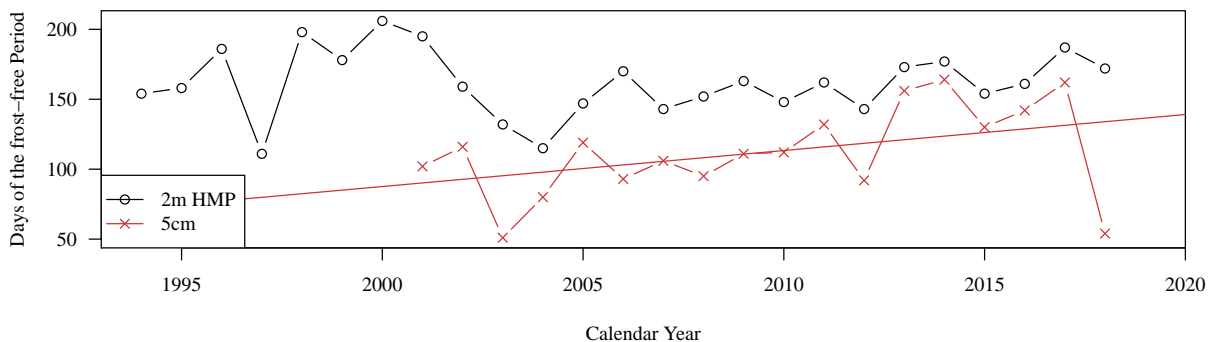


Figure 29: Number of days of the frost-free period at the EBG station. The 2 m height measurement is shown in black, the 5 cm height measurement in red. A linear regression line is depicted additionally, as there appears a significant trend in the 5 cm measurements.

At the 2 m height measurement, there occurs no trend towards a longer frost-free period. However, at the 5 cm height measurement, a positive trend was found. The last value in year 2018 seems to be an outlier. This outlier is caused by the very early first frost day at the 26th August 2018. Testing for a trend including this value, nevertheless, a significant positive trend towards a longer frost-free period is the result, with a rate of

2.5 and $p = 0.034$.

Comparison of the three different measuring stations

In the following, the length of the frost-free period is compared for the stations at the EBG, the Voitsumra and the Waldstein Container site.

Figure 30 shows the length of the frost-free period during the measuring period for the three measuring stations.

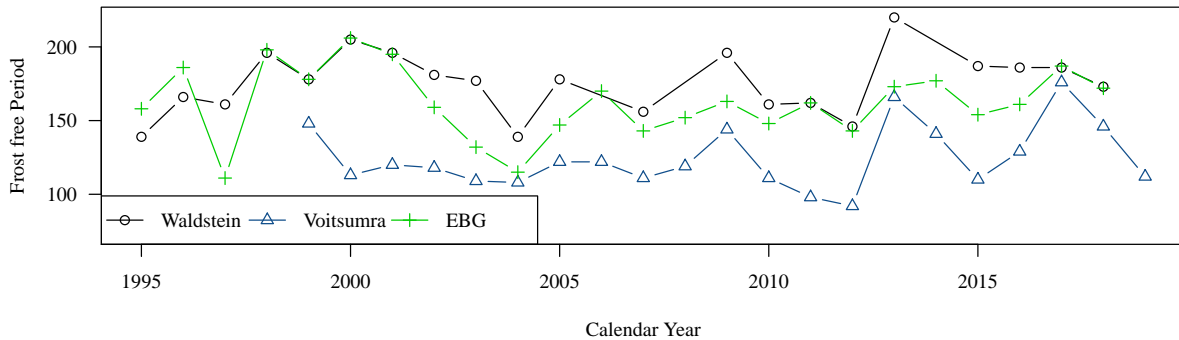


Figure 30: Comparison of the length of the frost-free period between the three stations. The Waldstein station is shown in black, the Voitsumra station in blue and the EBG station in green.

The frost-free period is shortest at the Voitsumra site with averaged 125 days and longest at the Waldstein site with averaged 175 days. This observation is consistent with the other findings, such as more occurring frost days at the Voitsumra site (see section 3.2.2).

The suggested trend towards longer frost-free periods during time were not confirmed by the Mann-Kendall trend test.

3.2.5 Interrelationships among Indices and Comparison to regional trends

In the following, it is analysed if there is a correlation between the mean frost period temperature and the number of frost days per winter.

In figure 31, the absolute number of frost days per winter year is plotted versus the mean frost period temperature for all three measuring sites.

There is a significant negative correlation between the mean frost period temperature and the number of frost days per winter year. For the Waldstein Container measurement this correlation is the highest. With a low mean winter temperature, many frost days occur, with a higher mean winter temperature, fewer frost days occur.

This was examined with the Pearson's product-moment correlation test. According to this test, at the EBG, there is a significant negative correlation with a correlation coefficient of -0.82 and $p < 0.001$ (linear equation: $y = 150.85 - 13.70 \cdot x$). For the Voitsumra measurement, there is a significant negative correlation with a correlation

3. RESULTS

coefficient of -0.74 and $p < 0.001$ (linear equation: $y = 155.22 - 10.47 \cdot x$). For the Waldstein Container measurement, there is a significant negative correlation with a correlation coefficient of -0.91 and $p < 0.001$ (linear equation: $y = 129.14 - 13.44 \cdot x$). This correlation is the highest as the correlation coefficient is closest to 1. So for all three measurements, the correlation between the mean frost period temperature and the number of frost days is significant at higher than a 99% level of confidence.

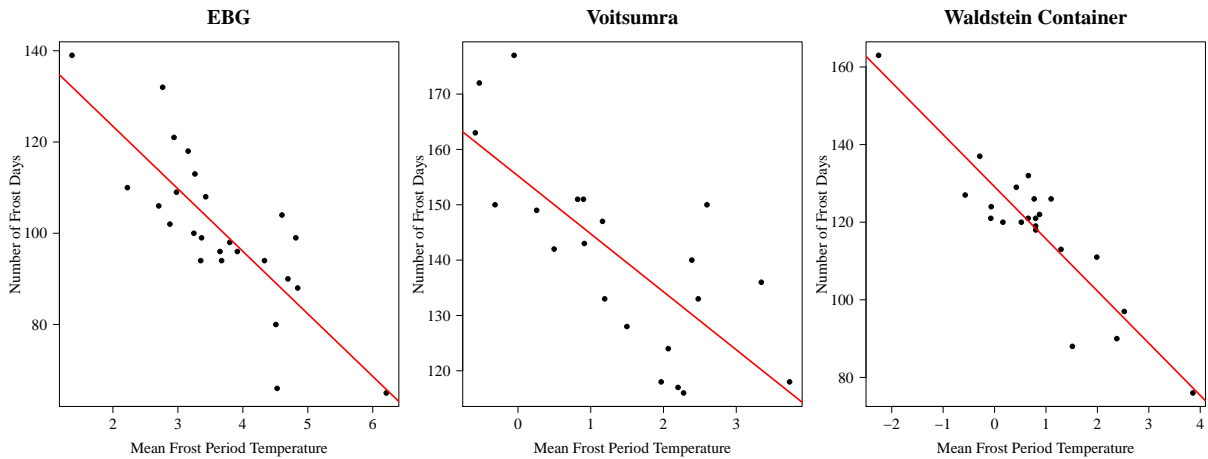


Figure 31: Scatterplot of the the number of frost days versus mean frost period temperature at the EBG, Voitsumra and Waldstein site. A linear regression line is shown additionally in red.

The correlation between the number of frost days and the mean frost period temperature shows the connection between the occurrence of frost days and the general occurring temperature during the mean frost period (and therefore the synoptic weather situation). This means that the respective micro-climate influences the Voitsumra site most. Therefore, this station is more independent from the general trend. This can also be said for the EBG, but to a lower extent.

At the Waldstein Container site there occurs the highest correlation between the number of frost days and the mean frost period temperature. Thus, this site is more affected by the general weather situation (and less by micro-climatic conditions) than the other two stations.

So, the number of frost days is linked to the mean frost period temperature, which is increasing at least for the Waldstein site. Thus, this additionally reveals that around 10 to 13 less frost days occur per °C higher mean frost period temperature. It is expected, that the increasing mean frost period temperatures will lead to a smaller number of frost days per winter year, which is consistent with the expectations based on the literature research. There is no detectable (significant) trend at the Voitsumra and the EBG site.

The same correlation analysis was done for the number of ice days with the mean frost period temperature. This analysis is shown in the Appendix in figure 59, the results are mentioned additionally in table 2.

3. RESULTS

Table 2: Summary table of the discovered correlations between climatological frost indices. The correlation coefficient is mentioned with the respective p-value in parenthesis. The rate of the linear regression is mentioned as well, otherwise "NA" is written.

First Indices (x-axis)	(x-indices)	Second Indices (y-axis)	EBC	Voitsumra	Waldstein
Bavarian of Frost Days	Average	Frost Days	0.46 (p = 0.023), rate = 0.61	0.63 (p = 0.003), rate = 0.85	0.56 (p = 0.005), rate = 0.74
Bavarian of Ice Days	Average	Ice Days	0.71 (p < 0.001), rate = 0.69	0.72 (p < 0.001), rate = 1.3	0.7 (p < 0.001), rate = 1.3
Mean Frost Period Temperature	Period	Frost Days	-0.82 (p < 0.001), rate = -13.7	-0.74 (p < 0.001), rate = -10.5	0.91 (p < 0.001), rate -13.4
Mean Frost Period Temperature	Period	Ice Days	-0.85 (p < 0.001), rate = -9.8	-0.68 (p = 0.002), rate = -11	-0.91 (p < 0.001), rate = -14.9
Frost Days		Ice Days	0.66 (p < 0.001), NA	0.60 (p = 0.006), NA	0.82 (p < 0.001), NA
Frost Events	Mean Length	Event	-0.65 (p < 0.001), NA	-0.78 (p < 0.001), NA	-0.82 (p < 0.001), NA

Comparison to regional trends

The German meteorological service is collecting the number of frost and ice days for all the federal states of Germany since 1951. Therefore, it is possible, to illustrate the number of frost days for Bavaria and Germany (see in figure 32) and to compare them to the measured frost days at our three meteorological stations.

The average number of frost day is always higher for Bavaria than for entire Germany. Moreover, the number of frost days shows a decreasing trend for Bavaria as well as for Germany. A significant negative trend in the frost days in Bavaria with a rate of -0.36 and $p < 0.001$ was discovered using the Mann-Kendall trend test. This trend is reflected in the German average. A significant negative trend with a rate of -0.30 and $p = 0.0011$ was discovered.

However, this trend seems to be limited to the years before 2000, as no significant trend was detected in the period 2000 - 2019 (non-significant negative trend for the time period since 1995).

The correlation of the frost days between the stations and the Bavarian average is illustrated and compared below (figure 33).

3. RESULTS

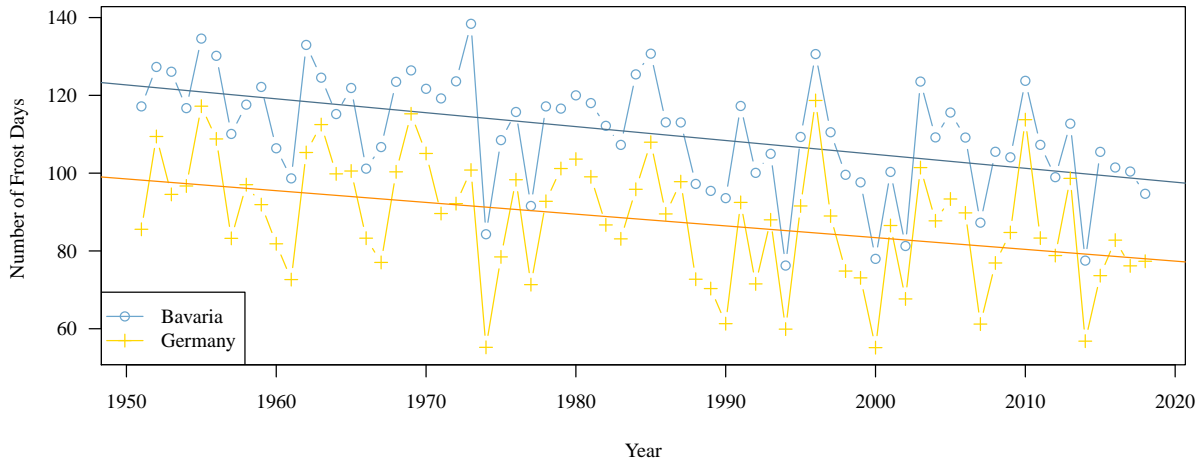


Figure 32: Absolute number of frost days for Bavaria (blue) and Germany (yellow). For both, a linear regression line is shown additionally, as there appear significant trends. Data provided by the German meteorological service (https://opendata.dwd.de/climate_environment/CDC/regional_averages_DE/annual/frost_days/)

The number of frost days of the respective station is plotted against the Bavarian average number of frost days. A line of equality (red) and a linear regression line (blue) were added. Here, it becomes visible that the number of frost days at the Voitsumra site is always much higher than the Bavarian average. On the contrary, the results of the EBG and the Waldstein site are a little more dispersed.

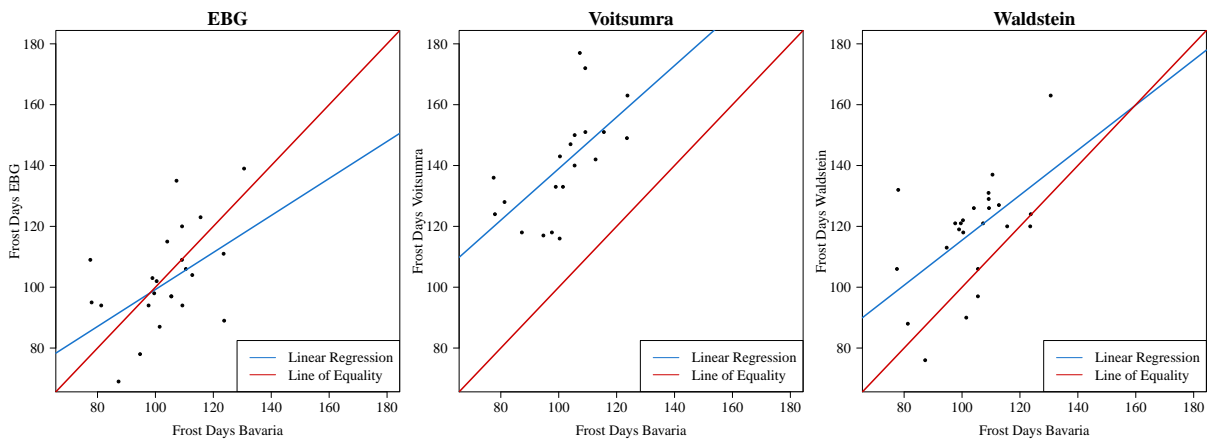


Figure 33: Scatterplots of the frost days measured at the meteorological stations versus the Bavarian average. A linear regression line is depicted in blue, a line of equality ($x=y$ line) in red.

For the EBG site a significant correlation with a correlation coefficient of 0.46 and $p = 0.023$ was discovered with the Pearson's product-moment correlation test. At the Voitsumra site a significant correlation with a correlation coefficient of 0.63 and $p = 0.0030$ was discovered. At the Waldstein site, a correlation with a correlation coefficient of 0.56 and $p = 0.0045$ was detected. Although these p-values are all significant, the correlation

3. RESULTS

coefficients are not particularly high (most suitable for the Voitsumra site).

In figure 34, the number of ice days averaged for Bavaria and Germany is shown. If the daily maximum temperature is below 0°C , the day is called an ice day.

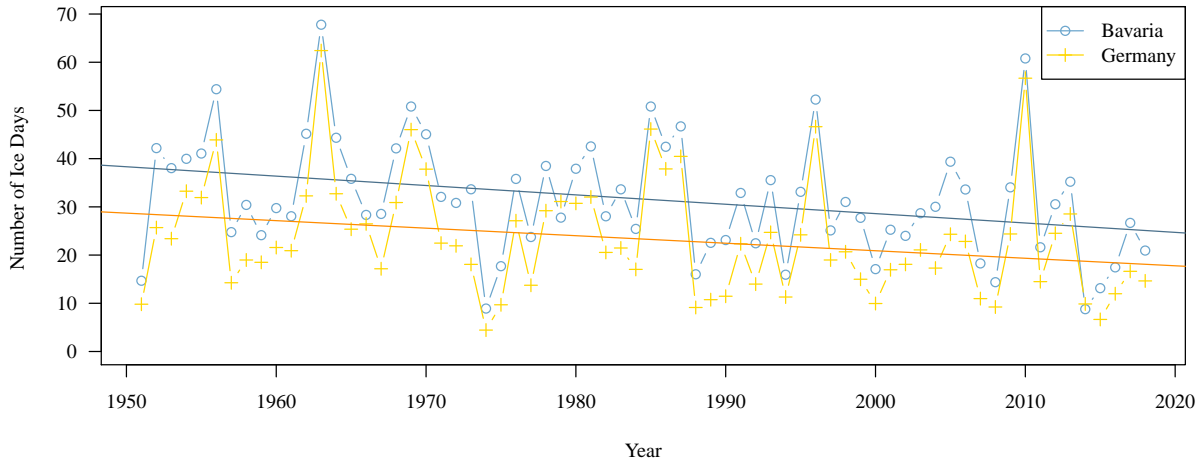


Figure 34: Absolute number of ice days for Bavaria (blue) and Germany (yellow). For both, a linear regression line is shown additionally, as there appear significant trends. Data provided by the German meteorological service (https://opendata.dwd.de/climate_environment/CDC/regional_averages_DE/annual/ice_days/)

It is shown, that the difference between the Bavarian and German average of ice days is smaller than for the frost days. Furthermore, there occur naturally less ice days than frost days. Here again, a decreasing trend in the number of ice days is observed. A significant negative trend was detected using the Mann-Kendall trend test with a rate of -0.19 and $p = 0.0045$ for Bavaria and a rate of -0.16 and $p = 0.015$ for entire Germany.

Similar to the number of frost days, these trends seem to happen before 2000, as no trend could be detected in the period 2000 - 2019, which is mainly the measuring period of the Voitsumra site. For the time period 1995 - 2019, which is the measuring period at the Waldstein and EBG site, only non-significant trends emerge.

The correlation of the ice days between the stations and the Bavarian average is illustrated and compared in figure 35.

Here, the points are not as scattered as for the frost days, and for the Voitsumra stations, the points are always higher than the Bavarian average as on the frost days.

At the EBG, a significant positive correlation was identified with a correlation coefficient of 0.71 and $p < 0.001$. At the Voitsumra site, a significant positive correlation was discovered with a correlation coefficient of 0.72 and $p < 0.001$. A significant positive correlation was also discovered at the Waldstein site with a correlation coefficient of 0.70 and $p < 0.001$. All these correlations are extremely significant and the coefficients are higher than for the correlation of the frost days.

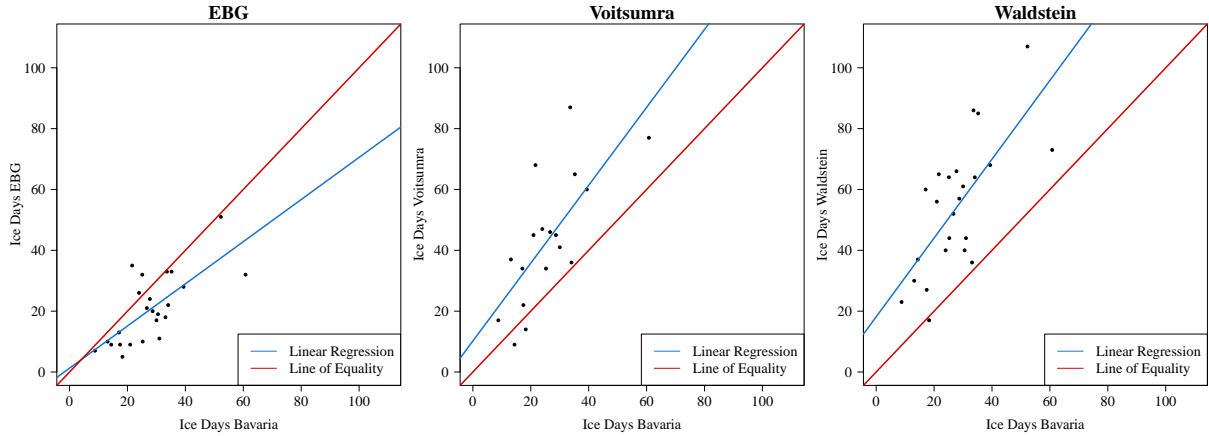


Figure 35: Scatterplot of the number of ice days of the three stations versus the Bavarian average. A linear regression line is depicted in blue, a line of equality ($x=y$) in red.

3.3 Frost Event based Statistics

3.3.1 The number of Frost and Ice Events

In the following the number of frost and ice events per winter year is depicted and described, first for the EBG and then in comparison of the three stations. A frost event is a continuous event of consecutive frost days, inter alia during which the daily minimum temperature is below 0°C . The time period of frost events can be one day or longer and between two frost events there have to be at least one day with the daily minimum temperature above 0°C . An ice event is an continuous event of consecutive days with the daily maximum temperature below 0°C .

Results of the EBG

The absolute number of frost and ice events per winter year is pictured in figure 36. The measuring instrument at 5 cm height is measuring the daily minimum, whereas, for calculating the ice days (and with them the ice events), the daily maximum is used. Thus, only ice days and events at 2 m heights were considered.

Although, there occur always more frost days at 5 cm height than at 2 m height, the number of frost events at 5 cm height can be below the number of frost events at 2 m height. This effect is due to a longer mean event length at 5 cm height compared with the mean event length at 2 m height (see section 3.3.2). The number of ice events is smaller with averaged 7 events than of the frost events with averaged 22 events per winter year. The number of frost and ice events are anti-correlated with a correlation coefficient of -0.50 and $p = 0.011$, meaning that if more frost events occur, less ice events occur.

With regards to a decrease or increase in the frost and ice events, no trend was detected using the Mann-Kendall test.

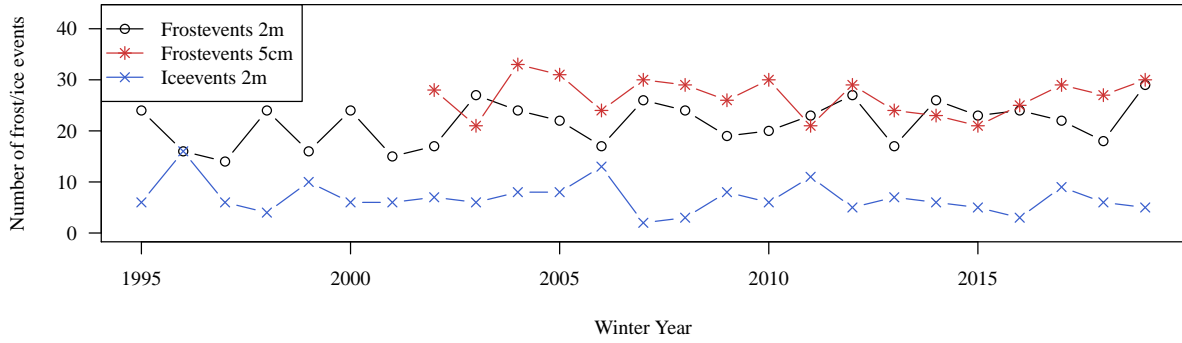


Figure 36: Absolute number of ice and frost events per winter in the EBG. The frost events at 2 m height are shown in black, those at 5 cm height are shown in red. The ice events are depicted in blue.

Comparison of the three different measuring stations

The number of frost events per winter year is shown for the three station in figure 37.

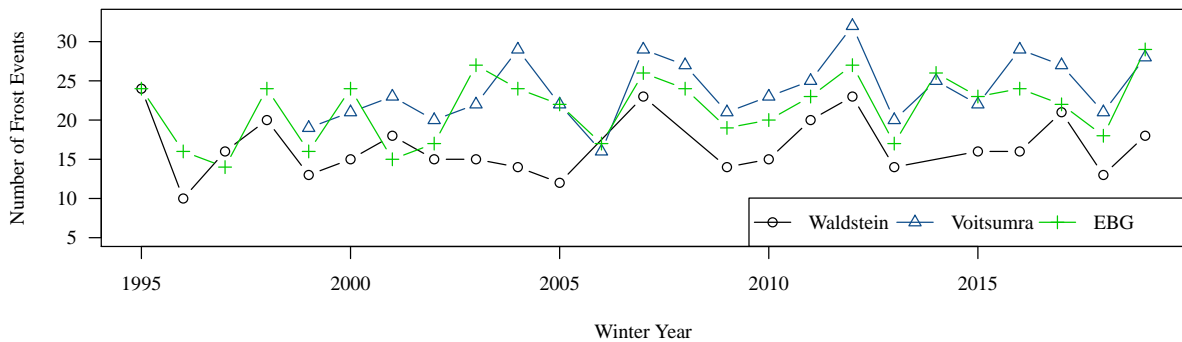


Figure 37: Comparison of the number of frost events between the three stations. The Waldstein station is shown in black, the Voitsumra station in blue and the EBG station in green.

The nearly always lowest number of frost events occurs at the Waldstein site with averaged 17 events. This observation can be explained by the fact that the mean frost event length is longest at this site (see section 3.3.2). With averaged 24 frost events per Winter year, the highest number of frost events occurs at the Voitsumra site. Between the Voitsumra and the EBG site, a positive correlation was detected using the Pearson’s product-moment correlation test. A correlation coefficient of 0.71 and $p < 0.001$ was detected. The EBG and the Waldstein site are less correlated with a correlation coefficient of 0.51 and $p = 0.015$. No correlation was discovered between the Voitsumra and the Waldstein site.

At the Waldstein site, the number of frost events seems to stagnate, whereas at the Voitsumra and the EBG site, it seems to ascend. However, no significant trends (e.g. towards a lower or higher number of frost events) occur at any station. Nonetheless, at the Voitsumra station, a non-significant positive trend towards a higher number of frost

events per winter year occurs with a rate of 0.25 and $p = 0.10$. At the EBG station, a similar non-significant trend appears with a rate of 0.21 and $p = 0.13$.

In figure 38 the number of ice events per winter is shown for the three different measuring stations.

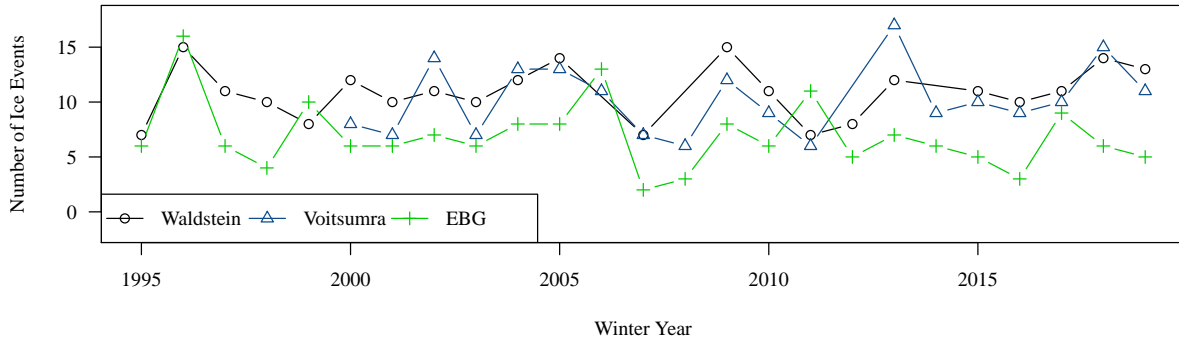


Figure 38: Comparison of the number of ice events between the three stations. The Waldstein station is shown in black, the Voitsumra station in blue and the EBG station in green.

The number of ice events per winter is lowest at the EBG site with averaged 7 events and it seems to stagnate. At the Voitsumra site and at the Waldstein site, the number of ice events is similar with averaged 10.21 or 10.86 events respectively. No significant trend towards a lower or higher number of ice events was discovered at any of the site using the Mann-Kendall trend test.

3.3.2 Mean Event Length

Results of the EBG

In the following, the mean number of frost days per frost event or the mean event length is shown and described. An overview of this variable at the EBG site throughout the winter years from 1995 to 2019 is shown in figure 39.

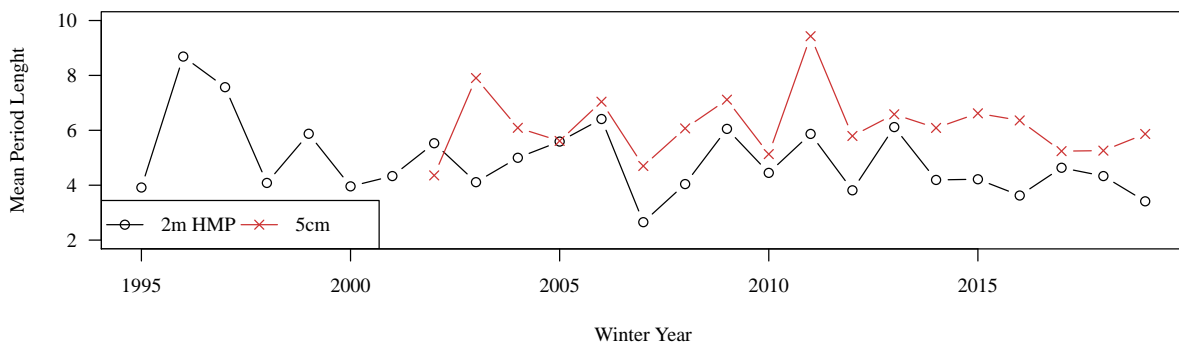


Figure 39: Mean frost event length in days per event at the EBG site. The mean frost event length at 2 m height are shown in black, those at 5 cm height is shown in red.

3. RESULTS

Here, one can see that the mean event length is higher at the 5 cm measurement with averaged 6.18 days than at the 2 m measurement with averaged 4.89 days. This observation fits with the finding that there are more frost days measured at 5cm height (averaged 162 days) than at the 2m measurement (averaged 101 days), but less more frost events (averaged 27 events versus averaged 22 events).

Comparison of the three different measuring stations

In figure 40 the mean frost event length is pictured for the three different measuring stations for comparison.

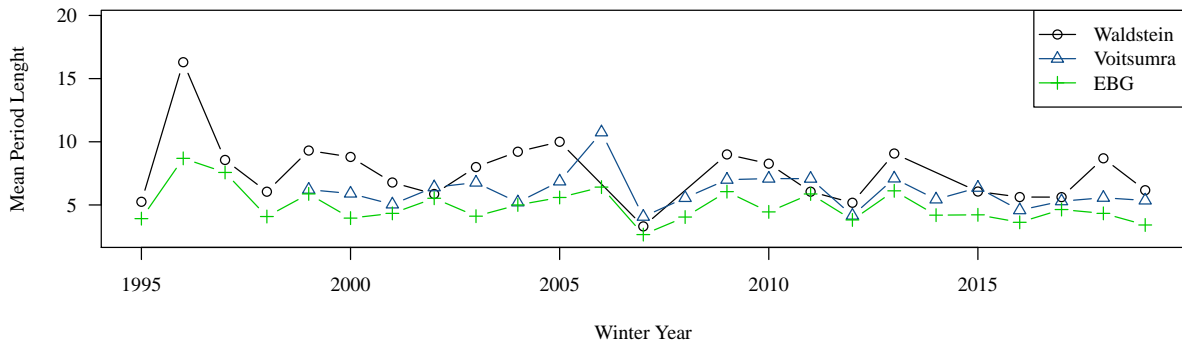


Figure 40: Comparison of the mean frost event length in days per event between the three stations. The Waldstein station is shown in black, the Voitsumra station in blue and the EBG station in green.

The mean frost event length does not differ that much between the three sites with 2.7 days as maximum difference of the averages. Nevertheless it is mostly smallest at the EBG site with averaged 4.9 days and largest at the Waldstein site with averaged 7.6 days. This order corresponds with the altitude order of the stations. Analyzed with the Mann-Kendall trend test, no any significant trends were detected.

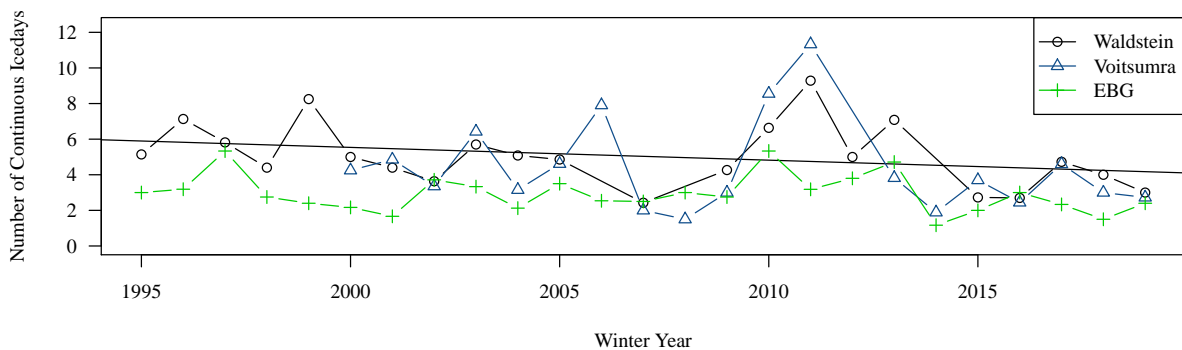


Figure 41: Comparison of the mean ice event length in days per event between the three stations. The Waldstein station is shown in black, the Voitsumra station in blue and the EBG station in green.

In figure 41 the mean ice event length (i.e. the mean number of ice days per ice events)

is shown for the three meteorological stations.

The mean ice event length is generally shorter than the mean frost event length with averaged 5.1 days at the Waldstein, 4.4 days at the Voitsumra and 2.9 days at the EBG site. This observation is consistent with the findings for the number of frost and ice events (lower number of ice events) and the number of frost and ice days (lower number of ice days).

At the Waldstein Container site, a trend towards shorter mean ice events occurs with a rate of -0.072 and $p = 0.063$. No trends were observed for the other two sites.

3.3.3 Maximum continuous ice event

The maximum continuous ice event describes the highest number of consecutive days with the daily maximum temperature below 0°C . Since the instrument at 5 cm height at the EBG station only measures the daily minimum, which is not used for the calculation of ice days and ice events, the results are directly compared between the three stations.

In figure 42 the maximum continuous ice event (or the longest continuous time period with no temperature above 0°C) is pictured for the three sites.

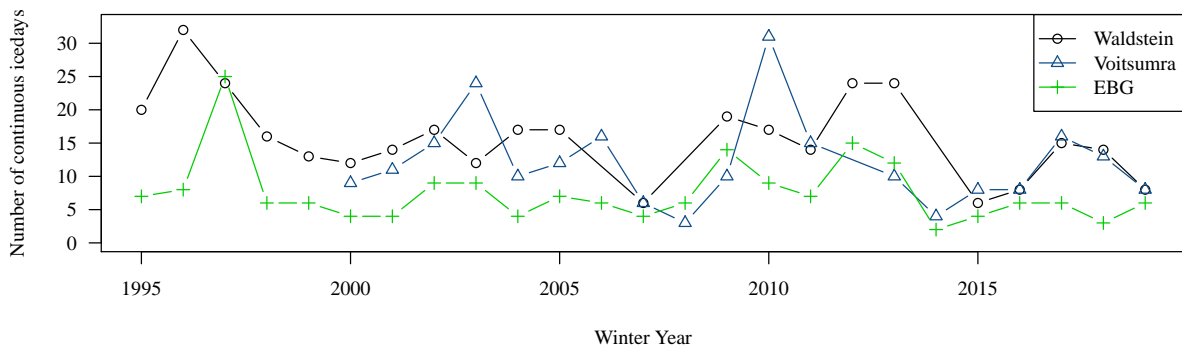


Figure 42: Comparison of the maximum continuous ice events in days per event between the three stations. The Waldstein station is shown in black, the Voitsumra station in blue and the EBG station in green.

It is apparent that the maximum continuous ice event is all in all shortest at the EBG site with averaged 7.6 days. At the Waldstein site with averaged 15.9 and the Voitsumra site with averaged 12.1 days, the maximum continuous ice event is longer. Nonetheless, there does not seem to be a specific order between the three sites that defines the site with longest or shortest maximum continuous ice events, respectively.

While there does not seem to be a trend at the Voitsumra site and at the EBG site (and checked with the trend tests, there could not be one detected), the maximum continuous ice period seems to get shorter over the time at the Waldstein site. There is a non-significant negative trend towards a shorter maximum continuous ice event with a rate of -0.34 and $p = 0.13$.

3.4 Comparison of the annual frost statistics with phenological events

The begin of the vegetation period is a variable that can be used to draw conclusions with regards to the frost risk. Thus, the begin of the vegetation period, as this is the period, where the frost damage can be severe for plants was calculated. The vegetation period starts phenologically with the bud break and the leaf unfolding and ends with the leaf drop (Larcher, 1984). But there are several other methods to calculate the thermal vegetation period (see section 3.4.2).

In the temperate climate zone, the date of the occurring of phenological phases/events is mainly dependent on the exceeding of specific temperature thresholds. In general, the temperature threshold for the bud break and the blooming is at 6-10°C and for crops around 15°C (Winkler, 1980). Frich et al. (2002) defined the "Growing Season Length" as the period between the thresholds daily mean temperature above 5°C for longer than 5 days and daily mean temperature below 5°C for longer than 5 days. For the main vegetation period (during which the majority of plants assimilate), a threshold of +10°C is used (Winkler, 1980).

3.4.1 Trends in the Phenological Spring Data

The analysis of the occurrence dates of phenological spring events is described in the following. The data is from the German meteorological service stations Weißenstadt and Aichig. At the Aichig station (data from 1981 or 1991 to 2017), no trends emerged (confirmed with the Mann-Kendall trend test, not shown). However, at the Weißenstadt station (data from 1951/1961/1991 to 2017), significant trends towards advancing occurrence dates of phenological spring events among several plants occur.

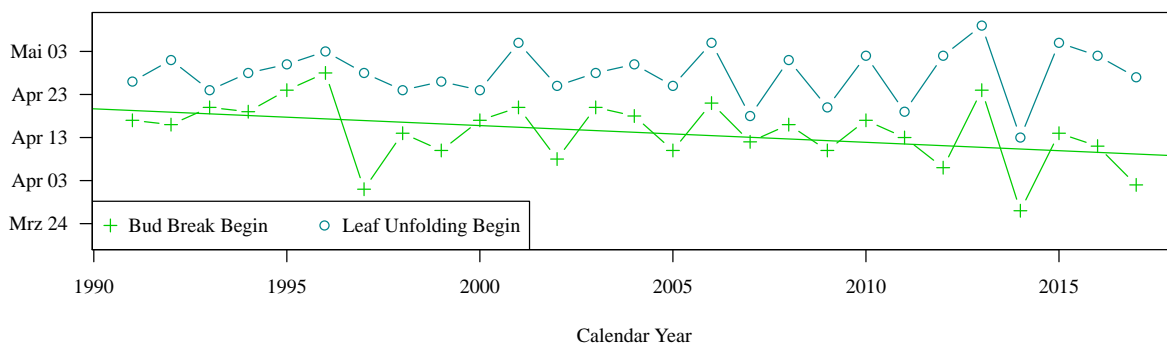


Figure 43: Date of the bud break begin and of the leaf unfolding begin of the mountain ash (Eberesche) at the site Weißenstadt. The bud break begin is shown in green, the leaf unfolding begin in blue. A linear regression line for the bud break begin is plotted additionally, as there occurs a significant trend. Data provided by the German Meteorological Service (https://opendata.dwd.de/climate_environment/CDC/observations_germany/phenology/annual_reporters/wild/historical/)

3. RESULTS

In figure 43 the date of the begin of the bud break and the leaf unfolding is pictured for the mountain ash at the site Weißenstadt.

Here, it appears that the leaf unfolding is not advancing but that the begin of the bud break is getting earlier. This could be confirmed by using the Mann-Kendall trend test, with which a significant negative trend towards an earlier beginning of the bud break with a rate of -0.39 and $p = 0.054$ was detected.

In figure 44 the phenological spring event leaf unfolding begin measured for the copper beech (Rotbuche) at the station Weißenstadt is pictured.

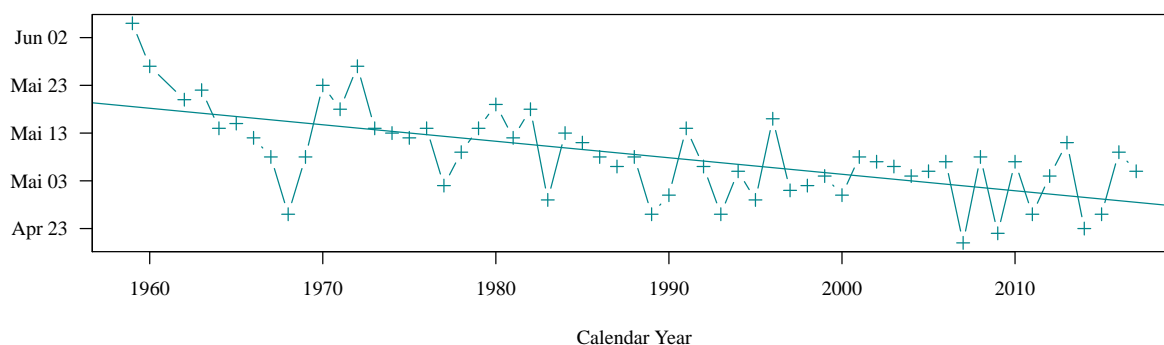


Figure 44: Date of the leaf unfolding begin of the copper beech (Rotbuche) at the site Weißenstadt. A linear regression line is plotted additionally, as there occur a significant trend. Data provided by the German Meteorological Service (https://opendata.dwd.de/climate_environment/CDC/observations_germany/phenology/annual_reporters/wild/historical/)

The measuring period is here from 1959 until 2017 and as for the measurement of the blooming begin of the mountain ash, which is measured in a similar time period, a strong trend occurs. A negative trend to earlier dates of the leaf unfolding begin was identified with a rate of -0.35 and $p < 0.001$ with the Mann-Kendall trend test.

Similarly, the trend of the blooming begin of the mountain ash at the station Weißenstadt is significant (figure 45).

The first thing to notice is that the begin of the blooming of the mountain ash is measured for a longer time period (1951 - 2017) than the bud break begin and the leaf unfolding begin of the mountain ash (1991 - 2017).

Nevertheless, the trend towards earlier blooming begin is even more clear than the trend towards earlier begin of the bud break. A significant negative trend was detected with a rate of -0.29 and $p < 0.001$ using the Mann-Kendall trend test. Thus, the beginning of blooming is advancing with -2.9 days per decade.

According to Lavoie and Lachance (2006), in southern Quebec the coltsfoot (Hufatich) blooms 15 - 31 days earlier at present than during the first part of the 20th century. As we do not have any phenological data for the coltsfoot before 1951, a direct comparison is not possible. However, a general trend analysis for the measuring period is reasonable.

3. RESULTS

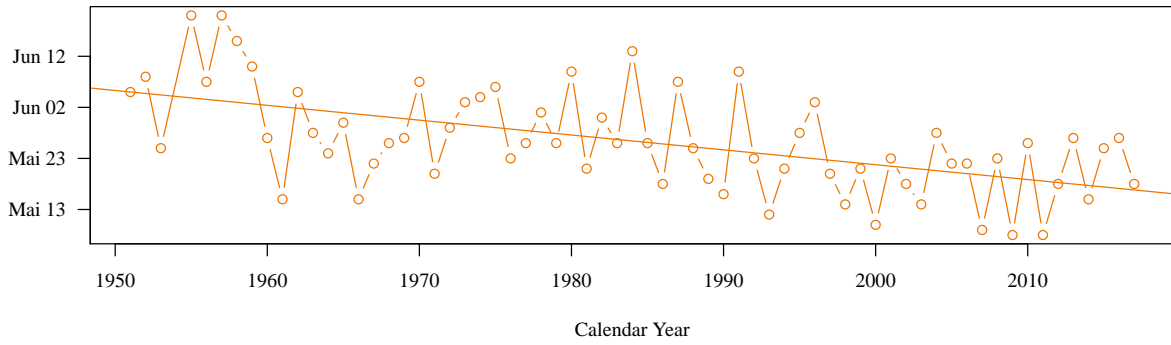


Figure 45: Date of the blooming begin of the mountain ash (Eberesche) at the site Weißenstadt. A linear regression line is plotted additionally, as there occurs a significant trend. Data provided by the German Meteorological Service (https://opendata.dwd.de/climate_environment/CDC/observations_germany/phenology/annual_reporters/wild/historical/)

In figure 46 the date of the phenological spring event blooming begin of the coltsfoot at the site Weißenstadt is pictured.

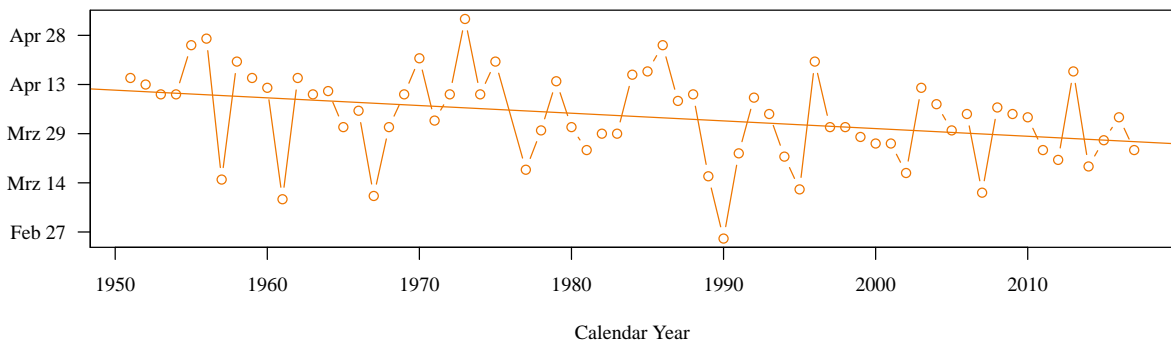


Figure 46: Date of the blooming begin of the coltsfoot (Hufflattich) at the site Weißenstadt. A linear regression line is plotted additionally, as there occurs a significant trend. Data provided by the German Meteorological Service (https://opendata.dwd.de/climate_environment/CDC/observations_germany/phenology/annual_reporters/wild/historical/)

Though the begin of the blooming is variable (standard deviation around 13 days), a negative trend towards earlier blooming begin dates was discovered with a rate of -0.23 and $p = 0.0010$ using the Mann-Kendall trend test.

At the Weißenstadt site, a non-significant trend towards earlier beginning of greening at the grassland was observed with a rate of -0.21 and $p = 0.13$. At the Aichig site, no significant trend was detected. However, as the measuring period is from 1991 to 2017, it is possible that the measuring period is too small to detect a significant trend.

3.4.2 Comparison of the vegetation period

There are different approaches on how to define the vegetation period: Menzel and Fabian (1999) defined the vegetation period as the period between the first spring events (such as leaf unfolding) and autumn events (such as leaf coloring). They observed that, primarily driven by spring phenologies starting earlier in the year, the growing period is extending and has lengthened by 10.8 days since the early 1960s. (Chmielewski, 2007) examined the thermal vegetation period as the period during which the daily mean temperature is above 5°C. A lengthening of 25 days in the period 1961 to 2005 was discovered. Frich et al. (2002) defined the 'growing season length' as the period between the thresholds daily mean temperature above 5°C for longer than 5 days and daily mean temperature below 5°C for longer than 5 days. In Winkler (1980) the main vegetation period is defined as period with the daily mean temperature above 10°C.

Due to the fact that several approaches were used to define the vegetation period, different length and trend rates were discovered in the literature. With the temperature data from the meteorological stations the growing season length according to Frich et al. (2002) and the main vegetation period according to Winkler (1980) was calculated. With the phenological data from the German meteorological service stations, the phenological vegetation period was calculated as described in Menzel and Fabian (1999). For these calculations, the daily mean temperature from data sets with corrected and filled mean temperature data were used, as they are longer and more consistent than the original temperature data sets.

Frich et al. (2002) detected a positive trend towards a longer growing season length, significant at the 95% level of confidence. Therefore, the thermal growing season length, calculated at the three meteorological measuring stations, was examined for trends (not shown). However, no significant trends nor non-significant trends were detected.

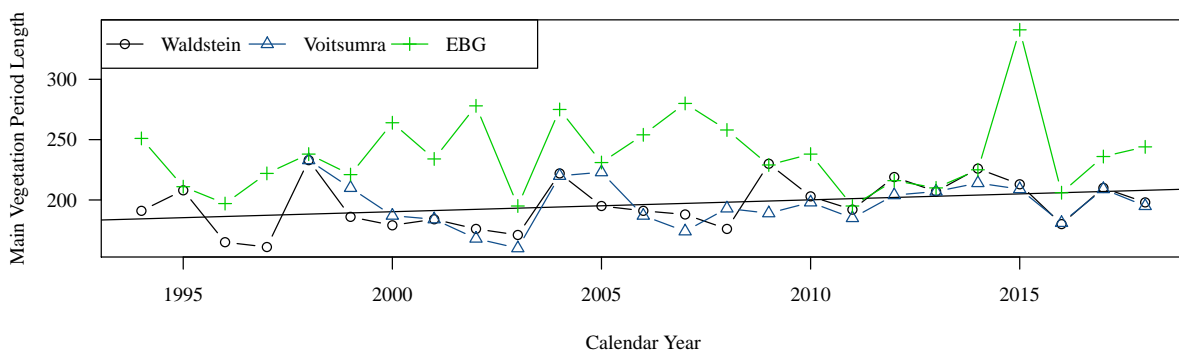


Figure 47: Comparison of the main vegetation period length between the three stations. The Waldstein station is shown in black, the Voitsumra station in blue and the EBG station in green. A linear regression line is shown additionally for the Waldstein station, as there occurs a significant trend.

Additional to this, the length of the main vegetation period ($T_{\text{mean}} > 10^{\circ}\text{C}$) was

3. RESULTS

calculated according to Winkler (1980). In contrast to the calculated growing season length, the main vegetation period length is showing a significant positive trend at the Waldstein Container site (see in figure 47).

At the EBG, the main vegetation period length is longest with averaged 238 days. At the Waldstein and the Voitsumra site, the results are similar with both averaged 196 days and positive correlated with a correlation coefficient of 0.71 and $p < 0.001$. At the EBG site and the Voitsumra site, there is no significant trend detectable. However at the Waldstein Container site, there was a significant positive trend detected towards a longer main vegetation period length with a gradient of 0.99 and $p = 0.079$. This trend is driven by the increasingly early begin of the thermal main vegetation period (figure 48).

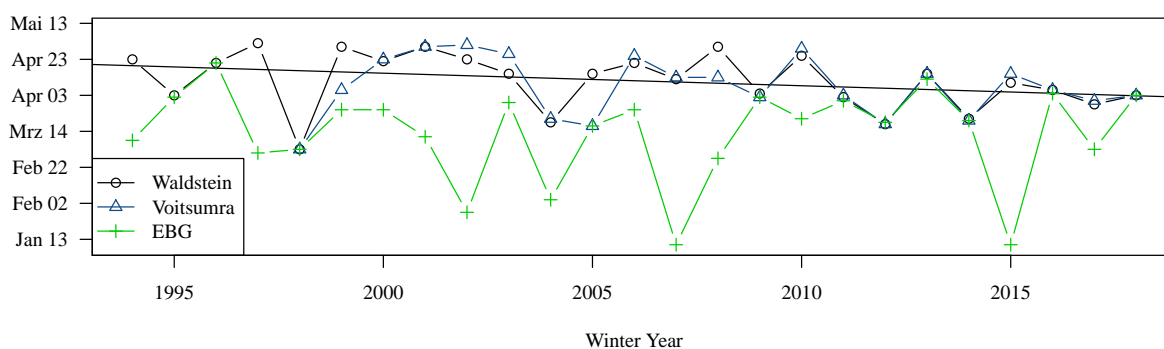


Figure 48: Start of the main vegetation period between the three stations. The Waldstein station is shown in black, the Voitsumra station in blue and the EBG station in green. A linear regression line is shown additionally for the Waldstein station, as there occurs a significant trend.

At the Waldstein Container site, there is a significant negative trend towards an earlier begin of the thermal main vegetation period with a gradient of -0.70 and $p = 0.0245$. The trend to a longer main vegetation period length is exclusively driven by this trend towards an earlier begin of the main vegetation period, as there is no significant trend to a later end of the main vegetation period. Similar to the calculation of the main vegetation period length, neither at the start nor at the end of the main vegetation period detectable trends occur at the Voitsumra and the EBG site.

The two different approaches to calculate the growing season length and the main vegetation period were compared in the following. At the EBG site the differences were small (figure 49) as the averages of both calculations are 238 days. An exception is the year 2015, in which the first day with the daily mean temperature above 10°C was in January.

Both at the Voitsumra and at the Waldstein site, the differences between the two calculations were greater compared to the EBG site with a difference between the averages of the two calculations of 18 days at the Voitsumra site and 10 days at the Waldstein site (not shown).

3. RESULTS



Figure 49: Comparison of the growing season length and the main vegetation period length at the EBG station. The growing season length is shown in light turquoise, the main vegetation period length in dark turquoise.

By comparing the calculated thermal growing season length or the main vegetation period with the vegetation period calculated with the phenological date, it becomes clear, that the real phenological vegetation period is always shorter than the thermal vegetation period at the EBG/Aichig site (not shown). The average of the growing season length and the main vegetation period is 238 days, whereas the average of the phenological vegetation period is 182 or 180 days for the mountain ash or the copper beech respectively.

This difference between the thermal and the phenological calculations is smaller at the Voitsumra and the Weißenstadt stations (figure 50).

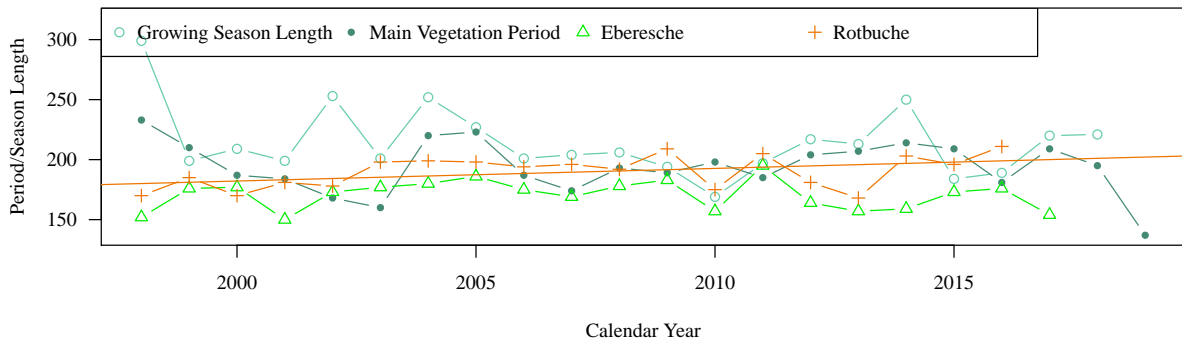


Figure 50: Comparison of the growing season length and the main vegetation period length with the phenological vegetation period at the Voitsumra/Weißenstadt site. The growing season length is shown in light turquoise, the main vegetation period length in dark turquoise. The phenological vegetation period of the mountain ash (Eberesche) is shown in green and those of the copper beech (Rotbuche) in orange. Phenological data provided by the German Meteorological Service (https://opendata.dwd.de/climate_environment/CDC/observations_germany/phenology/annual_reporters/wild/historical/)

The average of the growing season length is 214 days, of the main vegetation period 197. The average of the phenological vegetation period length is 171 for the mountain ash and 190 for the copper beech. Thus, the difference between growing season length or main vegetation period and the phenological vegetation period is smaller than at the

EBG site. However, the difference between the phenological vegetation period of the two examined plants is larger than at the EBG site (19 days versus 2 days).

Furthermore, the phenological vegetation period of the copper beech (Rotbuche) shows a positive trend to a longer vegetation period. The phenological vegetation period is lengthening with a trend rate of 11 days per decade ($p = 0.013$).

3.4.3 Frost Risk Analysis

According to Schwartz et al. (2006), if the difference in time between the onset of plant growth and subsequent last spring frost increases, the potential for damage increases, as plants are in more advanced stages of development. In addition to that, relative shifts in the timing of leaf unfolding versus timing and intensity of frost events determine whether frost risk changes under climate warming (Bigler and Bugmann, 2018).

Therefore, in the following, the phenological spring events are pictured together with the last frost day of the next meteorological station.

In figure 51 the phenological spring data of the mountain ash (bud break begin, leaf unfolding begin, blooming begin) is plotted along with the last frost day.

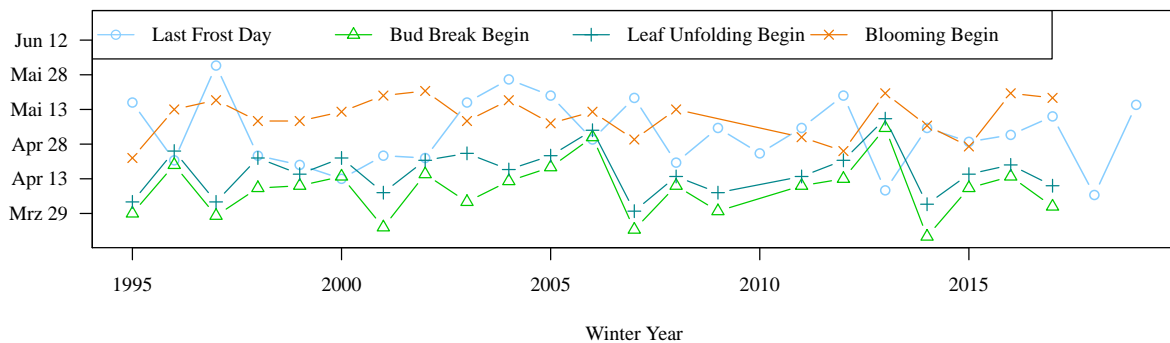


Figure 51: Phenological spring data of the mountain ash at the Aichig site and the last frost day at the EBG station. The last frost day is depicted in light blue, the bud break begin in green, the leaf unfolding begin in dark blue and the blooming begin in orange. Phenological data provided by the German meteorological service (https://opendata.dwd.de/climate_environment/CDC/observations_germany/phenology/annual_reporters/wild/historical/)

It appears that the last frost day mostly occurs after the beginning of bud break and leaf unfolding (with some exceptions, for example year 2014). In some years, the last frost day occurs even after the beginning of the blooming, which can cause frost damage at the plants.

Thus, as the the frost risk is increasing with an increasing time between the onset of phenological events and the last frost day (Schwartz et al., 2006), the difference between the phenological spring events and the last frost day was calculated. The results are discussed first for the EBG/Aichig site and then for the Voitsumra/Weißenstadt site.

3. RESULTS

At the EBG/Aichig site, no trend occurs in the difference between the last frost day and the phenological spring events of the mountain ash (not shown). For none of the plants, neither the copper beech, nor the coltsfoot or grassland significant trends towards larger differences between the occurrence of spring events and the last frost day were detected. Therefore, as no trends in the differences occur, the frost risk appears to stagnate.

At the Voitsumra/Weißenstadt site, though, trends towards smaller differences between last frost day and phenological spring events emerge. In figure 52 the phenological spring events of the mountain ash are shown along with the last frost day.

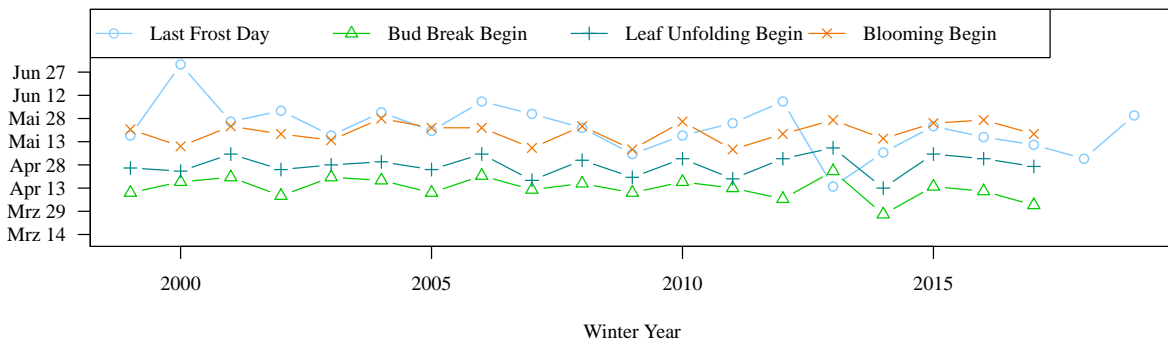


Figure 52: Phenological spring data of the mountain ash at the Weißenstadt station and the last frost day at the Voitsumra station. The last frost day is depicted in light blue, the bud break begin in green, the leaf unfolding begin in dark blue and the blooming begin in orange. Phenological data provided by the German meteorological service (https://opendata.dwd.de/climate_environment/CDC/observations_germany/phenology/annual_reporters/wild/historical/)

As the last frost day is advancing (with a rate of -11.9 days per decade, section 3.2.3), the difference between the occurrence of the phenological spring events and the last frost day is decreasing, entailing a decrease of the frost risk. The phenological spring events of the mountain ash at the Weißenstadt site are advancing since 1951 (‘blooming begin’) or since 1991 (‘bud break begin’). This trend to earlier occurring phenological spring events happened before 2000. Thus, during the examined period the occurrence dates of phenological spring events stagnate. Therefore, the difference is getting smaller for the leaf unfolding begin with a significant trend with a gradient of -0.36 and $p = 0.038$. A significant trend towards a smaller difference occurred as well for the beginning of blooming with a trend rate of -0.33 and $p = 0.058$. No significant trend emerged for the beginning of bud break (non-significant with rate = -0.35 and $p = 0.16$). The results for the examination of the other plants are similar, sometimes the trends to shorter differences are non-significant, sometimes they are significant.

According to these results, it appears that the frost risk is decreasing for the Voitsumra/Weißenstadt site. This is in large contrast to the results for the EBG/Aichig site, where the frost risk is stagnating. This difference in the results is probably driven by the fact, that at the EBG station, no trend to an earlier occurring last frost day at 2 m height

3. RESULTS

appeared. Hence, the development of the frost risk appears to be spatially heterogeneous.

4 Discussion

Due to climate change, the global mean temperatures are rising, especially in winter and spring. The effect of climate change is reflecting in climatological frost indices such as the number of frost days, which are significantly decreasing at a large scale. In order to analyse, how climate change is affecting climatological frost indices at a local scale, the following research questions have been formulated.

First of all, are there any significant trends in the mean winter temperature, the frequency and number of frost and ice events or the length of the continuous ice events per winter year? Moreover, are there significant trends in the coldest day in the year, first frost day in autumn and last frost day in spring and through that the length of the frost-free period? With regard to frost risk, are there significant changes in the trends of the advancing first frost day and the advancing of the phenological spring events and is this leading to a shift in the frost risk?

Second, how do the frost dynamics (frost days, ice days, etc.) and the possibly occurring trends differ between the different measuring stations? Further, which landscape characteristics and microclimatic conditions have an impact on these frost dynamics and could therefore cause these differences?

Between the three examined sites, there are several differences in the climatological frost indices. These differences are owing to the different microclimatic conditions and different landscape characteristics. Trends in the climatological frost indices occur spatially heterogeneous and mostly only at one site. The expected and discovered trends are discussed more detailed in the following. Afterwards, a table with a summary of the results is given (table 3).

Differences between the three sites

The most frost days occur at the Voitsumra site with an average of 141 frost days. The number of frost days is mostly similar at the Waldstein and the EBG site (17 days difference of the averages). The two sites are well correlated, with a correlation coefficient of 0.58 and $p = 0.005$, though, there is an altitude difference of 400 m between these two stations. The reason for this may be the different microclimatic conditions (Waldstein Container: surrounding coniferous trees, Voitsumra: strong cold-air influence). The minimum temperatures mostly occur at night, when the Voitsumra site is cold-air drainage influenced. At the Waldstein Container, the minimum temperatures occur at night as well, but they are relatively higher as this clearing station could be (to a certain extent) protected by the surrounding trees (long-wave outgoing radiation).

Consistent with these findings, the first frost day is often earliest at the Voitsumra site. The last frost day is at similar days at the EBG and the Waldstein site, which was not expected as there are 400 m difference in altitude.

Trends in temperature

According to Bonsal et al. (2001), the change in temperature is more pronounced for lower than for higher temperatures, and therefore more pronounced in winter and spring than in summer. This effect was described similarly by Sparks and Menzel (2002); Robeson (2004); Schwartz et al. (2006). The finding, that the change in temperatures is often larger in minimum than in maximum temperatures, is not reflecting in our results, see in figure 13 (noticed in Bonsal et al., 2001; Rochette et al., 2004). It was assumed, that a decrease in the frequencies of low temperatures would occur due to climate change. Furthermore, a uniform trend towards higher minimum temperatures was expected. At the EBG site, though, the change in temperatures appears to be larger in the daily maximum temperatures. The change in temperatures is showing no uniform trend. In the daily maximum temperatures at the Voitsumra site, the change is contrary to the expectation. A change towards lower temperatures occurring more frequently is observed (see in figure 14). At the Waldstein site, the change in the daily minimum temperatures is matching all in all the expectations. The lowest minimum temperatures are less often occurring in the second period and the frequencies for most temperatures below -2°C are decreasing (see in figure 15). This observation can explain, why the most trends in the climatological frost indices emerge at this site, compared with the other two sites. For the mean frost period temperature a significant trend towards higher temperatures was detected for the Waldstein site (increasing with 0.68°C per decade).

The value of the minimum winter temperature is interesting as according to Crumpacker et al. (2010) relatively large increases in the absolute minimum temperature can result in the invasion of nearby subtropical species into temperate systems. However, this is only to a certain extent transferable to our situation, since this investigation was model-based and in Florida. In Europe no subtropical system is directly bordered to the temperate system, in the south the Mediterranean system is attached. On the other hand, globalisation (e.g. tourism) could lead to subtropical plants also establishing themselves in Europe, provided that one of the dispersal barriers, such as the low minimum temperatures, would rise permanently. According to Bonsal et al. (2001), the daily minimum temperature increased significantly in the period 1900 to 1998 (over southern Canada). However, this does not match our results for the three stations. No trend emerged for any of the stations.

Trends in Frost and Ice Days

The increasing mean frost period temperature might influence the number of frost days. A decrease in the frost days was expected, as Frich et al. (2002) observed a significant decrease in frost days with a change of 5 - 15% between two multi-decadal averages during the 2nd half of the 20th century. Kiktev et al. (2003) found a significant (95% level of confidence) decrease of frost days with a rate of -2 to -4 days per decade for 1950 to

1995 for Europe. This is consistent with the calculated trend rate towards less frost days in the Bavarian average (rate of -3.6 days per decade) and the German average (rate of -3.0 days per decade). The trend at the Waldstein Container site is much larger. The number of frost days decreases significantly at the Waldstein site with a rate of -10 frost days per decade. However, since no significant trends emerged at the other two stations and in comparison with the literature, this discovered trend rate at the Waldstein site is large.

According to Kreyling and Henry (2011), there was a highly significant decrease of snow days (day with snow coverage $> 1\text{cm}$) per winter over the last 60 years. However, this observation was not transferable to the frost days at this local and temporal extent. Another possibility for no discovered trends in the frost days at the EBG and Voitsumra site is that the decrease of frost days could have already happened before the measurement started, as the examined period by Kreyling and Henry (2011) was from 1950 to 2000.

The ice days are decreasing in the Bavarian and German average as well. The difference between the Bavarian and German average of ice days is smaller than for the frost days. The ice days are less variable parameters than the frost days (lower standard deviation). Another explanation might be that the changes in lower (daily minimum) temperatures are larger than in higher (daily maximum) temperatures (observed in Bonsal et al., 2001; Scheifinger et al., 2003). However, at the meteorological stations, no trend emerged in the number of ice days. This might be caused by the short length of the measuring period. Furthermore, the trend in the Bavarian and German averages occurs mainly before 2000.

At the comparison and correlation analysis of the number of frost and ice days of the stations with the Bavarian average, the points were very scattered for the frost days. For the ice days, though, the points were less scattered and the correlation coefficients were higher. This implies that the daily maximum temperature (with which the ice days are calculated) depends more strongly on the general weather situation than the daily minimum temperature, which apparently depends more on the microclimatic conditions (see in table 2).

This finding is supported by the correlation analysis between the number of frost days and the mean frost period temperature. At the Waldstein Container site, the highest correlation between the number of frost days and the mean frost period temperature occurs. Thus, this site is more affected by the general weather situation (and less by microclimatic conditions) than the other two stations (see in table 2). At the Waldstein site, the mean frost period temperature is increasing, meanwhile the number of frost days is decreasing. It is expected, that the increasing mean frost period temperatures will lead to a smaller number of frost days per winter year, which is consistent with the expectations based on the literature research. There is no detectable (significant) trend in the number of frost days at the Voitsumra and the EBG site. This could be due to the short measuring period. However, a trend may emerge if the measuring period is

extended.

A decreasing trend in the number of frost and ice days will probably emerge in future, as especially the winter temperature is likely to rise and the mean frost period temperature is linked to the number of frost and ice days (shown in the correlation analysis in table 2).

Table 3: Summary table of the discovered trends at the measurement sites. Unit is "days per decade" unless otherwise noted. Trends significant at a 95% level of confidence are mentioned in bold. Non significant trends are mentioned with the respective p-value in parenthesis. If no trend appeared, "/" is written. Trends in the 5cm measurement of the EBG are mentioned in parenthesis.

Climatological Frost Indices	Expected Trends (Source)	EBG (5cm)	Voitsumra	Waldstein
Mean Frost Period Temperature (°C)	/	0.48 (p = 0.14)	/	0.68
Number of Frost Days	- 5 to 15% (Frich et al., 2002), -2 to -4 (Kiktev et al., 2003)	/	/	-10
Number of Ice Days	/	/	/	/
Minimum Temperature (°C)	up to + 4 (Bonsal et al., 2001, Period 1999-1998)	/	/	/
First Frost Day	2 (Bonsal et al., 2001)	/ (15)	/	/
Last Frost Day	up to 5 (Bonsal et al., 2001), 1.5 (Schwartz et al., 2006), 2.2 (Scheifinger et al., 2003)	/ (-15)	-12	/
Frost-free Period	up to 5 (Bonsal et al., 2001), 4.9 (Menzel et al., 2003)	/ (25)	/	/
Frost Events (Number of Events)	/	2.1 (p = 0.13)	2.5 (p = 0.10)	/
Ice Events (Number of Events)	/	/	/	/
Mean Ice Event Length	/	/	/	-0.7
Maximum continuous Ice Period	/	/	/	-3.4 (p = 0.13)

Bonsal et al. (2001) discovered a trend towards earlier last frost days with up to 5 days per decade (Canada, 1900-1998). According to Schwartz et al. (2006), the last frost day is advancing with a rate of 1.5 days per decade (northern Hemisphere, 1955-2002). Scheifinger et al. (2003) observed an advancing of the last frost day with a rate of averaged 2.2 days per decade (South Germany, 1951-1997). A significant trend is observed in the last frost day at a 5cm height in the EBG. The last frost day is getting earlier with 15

days per decade. Compared to the literature, the detected trend at 5 cm height exceeds the expected trend rate. For the Voitsumra station, a significant trend towards earlier occurring last frost days emerged as well. Here, the last frost day is getting earlier with 12 days per decade. All these trends mentioned in the literature are clearly lower than the trends identified in our analysis.

The frost-free period is lengthening for the 5cm height measurement in the EBG (trend rate of 25 days per decade). The discovered trend at the EBG 5 cm measurement coincides with the expected trend that, caused by earlier last frost day and later first frost day, the frost-free period is extending (Schwartz et al., 2006). However, in the literature mentioned trend rate for the lengthening of the frost-free period is 5 days per decade (Bonsal et al., 2001). Frich et al. (2002) observed that the period with no temperatures below 5°C for longer than 5 days (Growing Season Length, see section 3.4.2) is increasing with an average rate of 1.6 days per decade, while Menzel et al. (2003) found that the frost-free period is increasing with a rate of 4.9 days per decade. As the frost-free period has a very important impact on plants, as thermal growing period, an expansion could have an impact on the growing behavior of plants (Winkler, 1980).

Trends in the Frost Events

For the number of frost events and number of ice events, no significant trends emerge. For the mean ice period length, a significant trend towards shorter ice events occurred at the Waldstein site (trend rate of -0.71 days per decade). This might be caused by the increasing mean frost period temperature. For the maximum continuous ice period as well, no significant trends were detected. According to Rochette et al. (2004) more frequent winter thaw events would result in a loss of frost hardiness. So, if the number of frost and ice events increases, it means that more winter thaw events occur. However, for our stations, this does not seem to be transferable, as no trends to more or less frost events occur. All in all, the event based statistics do not appear to be that telling (especially frost event based).

Trends in Phenological Data and Frost Risk

As the degree of climate change in future is unknown, it is difficult to predict the further development of the frost risk and frost damage. The first appearance of spring foliage shows a strong response to temperature change (Schwartz et al., 2006). In order to analyse the frost risk at our local scale, phenological spring data was compared with the last frost day. A summarize of the expected and discovered trends is given in table 4.

The phenological data of the mountain ash, the copper beech, the coltsfoot and grassland and from 2 phenological stations, Weißenstadt and Aichig, was used.

According to Bigler and Bugmann (2018), leaf unfolding has been advancing across all species, particularly at higher elevations above 800 m. However, this is only conditionally

applicable for our situation, since the phenological stations are located at lower elevations.

Based on literature, phenological spring events like leaf unfolding, bud break or else have been occurring earlier in the year over the last decades. According to Schwartz et al. (2006), first leaf dates (for measuring 'early spring') are getting earlier with an average rate of -2.2 days per decade in Europe since 1955. Menzel (2000) noticed that leaf unfolding has advanced with a rate of -2.1 days per decade since 1959. First bloom dates (for measuring 'late spring') are occurring earlier with an average rate of -1.0 days/decade (Schwartz et al., 2006). According to Scheifinger et al. (2003), phenological spring events are getting earlier with at rate of up to -3 days per decade.

At the Weißenstadt station, the beginning of bud break of the mountain ash is getting significantly earlier with a trend rate of -3.8 days per decade. This trend is even higher than the trend discovered by Scheifinger et al. (2003). The beginning of blooming of the mountain ash is advancing with a trend rate of -2.9 days per decade. This trend rate is a lot higher than the expected rate of -1.0 days per decade, according to Schwartz et al. (2006).

The beginning of leaf unfolding of the copper beech is advancing with a trend rate of -3.4 days per decade. This trend rate is also about 1.2 days per decade higher than expected based on literature research (up to -2.2 days per decade, Schwartz et al., 2006).

Lavoie and Lachance (2006) examined inter alia the change of the occurrence of phenological spring events of the coltsfoot. In our phenological data, a significant trend towards an earlier beginning of blooming emerged with a trend rate of -2.3 days per decade. According to Bigler and Bugmann (2018), an advancement of the leaf unfolding occurs pronounced for higher elevations above 800 m. The two phenological stations are at lower heights, Aichig at 380 m above sea level and Weißenstadt at 620 m above sea level. However, trends in the phenological data emerge at a significant level at the Weißenstadt station, whereas no trends emerge at the Aichig station. However, this effect could also be caused by the shorter time series at the Aichig station.

A significant increase in the growing season length between 1951 and 1996 was observed (Frich et al., 2002). With the temperature data, the growing season length (according to Frich et al., 2002) and the main vegetation period (like in Winkler, 1980) was calculated for each meteorological station. In the growing season length, no trends emerged. In the main vegetation period, though, a significant trend towards a longer period occurs at the Waldstein site (trend rate of 9.8 days per decade). This is mainly driven by the advance of the main vegetation period. For the other two stations, no trend emerged.

For mountain ash and copper beech, phenological fall data was available, so the length of the phenological vegetation period was calculated. For the copper beech at the Weißenstadt site, a significant trend towards a longer main vegetation period was detected (trend rate of 11 days per decade). For the mountain ash at both stations, Weißenstadt and Aichig, no trend towards a longer period appeared.

Table 4: Summary table of the expected and discovered trends in the phenological data at the Weißenstadt station. Unit of trends is "days per decade" unless otherwise noted. Trends significant at a 95% level of confidence are mentioned in bold. Non significant trends are mentioned with the respective p-value in parenthesis. If no trend appeared, "/" is written. If the indices is not measured or not calculated "NA" is pictured.

Phenological Indices	Expected (Source)	Trends	Mountain Ash	Copper Beech	Coltsfoot
Bud Break Begin	NA		-3.9	NA	NA
Leaf Unfolding Begin	-2.2 (Schwartz et al., 2006), -2.1 (Menzel, 2000)	/		-3.5	NA
Blooming Begin	-1 (Schwartz et al., 2006)		-2.9	NA	-2.3
Phenological Vegetation Period	2.7 (Menzel and Fabian, 1999)		/	11	NA

The difference between phenological spring events and the last frost day is stagnating at the EBG/Aichig site, meaning that the frost risk is stagnating at this site. At the Voitsumra/Weißenstadt site, though, the frost risk is decreasing, due to the advancing last frost day. Schwartz et al. (2006) noticed that the relative rates of change of first leaf and last spring frost dates are spatially heterogeneous. These findings are consistent with our results. However, the phenological stations and the meteorological stations are not exactly at the same site, but within a distance of up to 2.3 km. Therefore, at the phenological station, the microclimatic conditions can be different to the conditions at the meteorological stations. Nevertheless, these results can give an approximate estimate about the development of the frost risk.

Summarized findings

In order to answer the research questions, in some climatological frost indices trends occur, mostly at the Waldstein or at the Voitsumra site. In the EBG, significant trends emerge only in the 5 cm height measurement. With regard to frost risk, at the EBG/Aichig site it is stagnating, while it is decreasing at the Voitsumra/Weißenstadt site.

Based on the literature, the expectations were that the general trend of increasing winter temperatures is exhibiting as well in the climatological frost indices at this local climate scale. Additionally, the number of frost days was expected to decrease as well as the number of ice days. The first frost days were assumed to show a delaying trend and the last frost days to show an advancing trend.

Further, it was expected, that the first frost day in fall is showing a delaying trend, while the last frost day in spring is getting earlier. This expectation was to some extent confirmed (see table 3). Mostly in the 5 cm height measurement in the EBG the expected trends occurred.

The climatological frost indices differ strong among the sites. In general, the occur-

rence of trends is spatially heterogeneous. Summarising, the EBG station is at the most warmest site (highest mean winter temperatures) compared with the other two sites. This observation is revealing in the number of frost days (fewest) and the number of ice days (always fewest) as well. It is probably caused by the fact that this station is the station at the lowest elevation.

The Voitsumra site is cold-air drainage/pooling influenced. This influence is reflecting in the frost indices (e.g. highest number of frost days per winter year), as the lowest daily temperature is generally occurring during nighttime. Consistently, the mean winter temperature is mostly lowest in Voitsumra (and as well the minimum temperature). No significant trends were detected, except for the last frost day in spring, which is advancing.

At the Waldstein Container site, which is a clearing surrounded by a conifer forest, the influence of the vegetation was recorded. For instance, the number of frost days is similar to the number of frost days at the EBG station, although the elevation difference between the two stations is 400 m. Additionally, the minimum temperature is sometimes even higher than at the EBG station. At this station, a significant trend towards a higher mean frost period temperature and a significant trend towards a lower number of frost days were detected.

At the Weißenstadt site, several trends towards earlier spring phenologies were discovered over a couple of plants. This finding means that the occurrence of phenological spring events is advancing. The calculated thermal main vegetation period is showing a lengthening trend at the Waldstein site with 9.9 days per decade. But this site is probably decoupled from the Weißenstadt station. The phenological vegetation period is mostly shorter than the calculated thermal vegetation period and for the copper beech at the Weißenstadt site, the phenological vegetation period is lengthening with a rate of 3.6 days per decade. With regard to frost risk, as the difference between the date of phenological spring events and the last frost day is stagnating for the EBG/Aichig site, but decreasing at the Voitsumra/Weißenstadt site, this leads to the assumption that the frost risk is stagnating for the EBG/Aichig site and decreasing at the Voitsumra/Weißenstadt site. The Voitsumra site appears to be the coldest site with regard to frost days. The site is mainly influenced by cold air drainage and pooling. This influence is reflecting in the climatological frost indices. For the ice days, the decoupling of this site is not that large.

The differences in the results and trends of the three stations are mostly caused by the influence of cold-air drainage and pooling in cloudless nights at the Voitsumra site. Supporting this, the number of ice days (calculated with the daily maximum temperature, which is usually occurring during daytime) is in several winter years equal or higher at the Waldstein site. The influence of the surrounding forest is appearing at the Waldstein site and probably causing, that the climatological frost indices are often similar to those calculated of the EBG site. The most trends are occurring at the Waldstein site.

Some of the expected trends were not reflected by our data. In this case, several

reasons might serve as explanation: Whereas a typical time period of measurements is 50 to 100 years (Frich et al., 2002; Bonsal et al., 2001; Scheifinger et al., 2003; Schwartz et al., 2006), our measuring period covers 20 - 25 years, starting earliest in the year 1994. Thus, significant trends might have occurred at our measuring sites before the start of our measurements. Furthermore, the research was often done for a completely different scale (e.g. northern Hemisphere, Europe Frich et al., 2002; Kiktev et al., 2003; Menzel, 2000). Thus, trends discovered in the average of many stations do not emerge at our local scale. Additionally, results from research that was conducted in foreign countries are not easily transferable to our data (e.g. Canada Kiktev et al., 2003).

At this point, it is necessary to discuss the limits of our data analysis. Compared with the reviewed literature, the analysed measuring period is short. Additionally, there are some gaps in the data. These gaps were filled with adjusted data from near measuring stations, nonetheless, this approach reduces the accuracy of the data and thus also the accuracy of the calculations.

5 Conclusion

The research questions, first if any trends occur in the examined climatological frost indices and if the frost risk is shifting and second, how and why the climatological frost indices differ between the stations, are reconsidered now. In some climatological frost indices, significant trends were discovered (see in table 3). These trends are spatially heterogeneous, meaning that if a trend occurs in an indices at one site, at the other two sites, no trend emerges. The spatial heterogeneity of the occurring trends is probably caused by the different landscape characteristics and microclimatic conditions.

However, in some climatological frost indices, no significant trends at any station emerged. This observation could be caused by the short measuring period, as in literature, minimum 30 years of consistent temperature data was used. However, a reason for no occurring trends can be also the data gaps and the reduced accuracy of the filled data. The data gaps and the reduced accuracy of the filled data can result in uncertainties in the found trends, as well.

Another possibility for not occurred but expected trends is that the increasing temperatures do not occur in this local and temporal scale, as there was no significant trend towards higher minimum temperatures detected. Nevertheless, some trends were detected despite the short time series. These early results suggest that the winter climate change indicators should be further analysed in the future, with more data supporting the analysis. Furthermore, the number of frost days is correlated with the mean temperature and the temperatures will likely rise onward (especially in winter and early spring). Thus, the data should be reanalysed for changes regarding these climatological frost indices in the future.

With regard to frost risk and frost damage of plants, further monitoring of the climatological frost indices together with phenological data is recommended. As a part of fundamental research, further analysis regarding changes and trends in the climatological frost indices is suggested, in particular with regard to the continuing climate change. Already occurring trends might intensify or new trends might appear under ongoing global climate change. Additionally, it is recommended to work with consistent valuable data. To investigate the influence of microclimatic conditions, one could examine the correlation between frost days or minimum temperature and the respective general weather situation. To exclude the uncertainty of different microclimatic conditions and to ensure the accuracy of the frost risk analysis, it is suggested to use stations where both meteorological parameters and phenological data are measured and collected.

References

- Bigler, C. and Bugmann, H. (2018). Climate-induced shifts in leaf unfolding and frost risk of European trees and shrubs. *Scientific Reports*, 8(1):1–10.
- Bonsal, B. R., Zhang, X., Vincent, L. A., and Hogg, W. D. (2001). Characteristics of daily and extreme temperatures over Canada. *Journal of Climate*, 14(9):1959–1976.
- Chmielewski, F.-M. (2007). Folgen des Klimawandels für Land- und Forstwirtschaft. *Der Klimawandel - Einblicke, Rückblicke und Ausblicke*, pages 75–85.
- Chmielewski, F. M. and Rötzer, T. (2002). Annual and spatial variability of the beginning of growing season in Europe in relation to air temperature changes. *Climate Research*, 19(3):257–264.
- Crumpacker, D. W., Box, E. O., and Hardin, E. D. (2010). Papers Implications of Native Trees Climatic Shrubs Warming in for Conservation of and. *Conservation Biology*, 15(4):1008–1020.
- DWD Climate Data Center (CDC) (2019a). Phenological observations of crops from sowing to harvest (annualreporters, historical), Version v006.
- DWD Climate Data Center (CDC) (2019b). Phenological observations of wild plants, including forest and ornamentalwoody plants from beginning of sprouting and flowering to ripening, also falling of leaves for some species(annual reporters, historical), Version v006.
- Foken, T. (2017). *Micrometeorology*. Springer-Verlag Berlin Heidelberg, 379 pages, 2 edition.
- Foken, T., Gerstberger, P., Köck, K., Siebcke, L., Serafimovich, A., and Lüers, J. (2017). Description of the Waldstein Measuring Site. In Foken, T., editor, *Energy and Matter Fluxes of a Spruce Forest Ecosystem*, chapter 2 Descript, pages 19–40. Springer International Publishing AG.
- Frich, P., Alexander, L. V., Della-Marta, P., Gleason, B., Haylock, M., Klein Tank, A. M. G., and Peterson, T. (2002). Observed coherent changes in climatic extremes during the second half of the twentieth century. *Climate Research*, 19:193–212.
- German meteorological Service (2019). Weather Encyclopedia.
- Jones, P. D. and Moberg, A. (2003). Hemispheric and Large-Scale Surface Air Temperature Variations: An Extensive Revision and an Update to 2001. *Journal of Climate*, 16:18.

- Kiktev, D., Sexton, D. M. H., Alexander, L. V., and Folland, C. K. (2003). Comparison of Modeled and Observed Trends in Indices of Daily Climate Extremes. *Journal of Climate*, 16:3560–3571.
- Klein Tank, A. M. and Können, G. P. (2003). Trends in Indices of daily temperature and precipitation extremes in Europe, 1946-99. *Journal of Climate*, 16(22):3665–3680.
- Kreyling, J. and Henry, H. A. (2011). Vanishing winters in Germany: Soil frost dynamics and snow cover trends, and ecological implications. *Climate Research*, 46(3):269–276.
- Larcher, W. (1984). *Ökologie der Pflanzen*. Eugen Ulmer GmbH & Co., 403 pages, Stuttgart, 4 edition.
- Lavoie, C. and Lachance, D. (2006). A new herbarium-based method for reconstructing the phenology of plant species across large areas. *American Journal of Botany*, 93(4):512–516.
- Loos, E. (2016). *Dynamics of the temperature and wind profiles in the boundary layer of a valley in the Fichtelgebirge Mountains*. Bachelor thesis, University of Bayreuth.
- Lüers, J., Soldner, M., Olesch, J., and Foken, T. (2014). 160 Jahre Bayreuther Klimazeitreihe Homogenisierung der Bayreuther Lufttemperatur- und Niederschlagsdaten von Johannes Lüers. Technical Report 56, University of Bayreuth.
- McLeod, A. (2011). *Kendall: Kendall rank correlation and Mann-Kendall trend test*. R package version 2.2.
- Menzel, A. (2000). Trends in phenological phases in Europe between 1951 and 1996. *International Journal of Biometeorology*, 44(March 2000):76–81.
- Menzel, A. and Fabian, P. (1999). Growing season extended in Europe. *Nature*, 397(6721):659–659.
- Menzel, A., Jakobi, G., Ahas, R., Scheifinger, H., and Estrella, N. (2003). Variations of the climatological growing season (1951-2000) in Germany compared with other countries. *International Journal of Climatology*, 23(7):793–812.
- Robeson, S. M. (2004). Trends in time-varying percentiles of daily minimum and maximum temperature over North America. *Geophysical Research Letters*, 31(4):1–4.
- Rochette, P., Bélanger, G., Castonguay, Y., Bootsma, A., and Mongrain, D. (2004). Climate change and winter damage to fruit trees in eastern Canada. *Canadian Journal of Plant Science*, 84(4):1113–1125.

- Scheifinger, H., Menzel, A., Koch, E., and Peter, C. (2003). Trends of spring time frost events and phenological dates in Central Europe. *Theoretical and Applied Climatology*, 74(1-2):41–51.
- Schönwiese, C.-D. (2013). Anthropogene Klimabeeinflussung. In *Klimatologie*, chapter 12 Anthrop, pages 336–377.
- Schwartz, M. D., Ahas, R., and Aasa, A. (2006). Onset of spring starting earlier across the Northern Hemisphere. *Global Change Biology*, 12(2):343–351.
- Sparks, T. H. and Menzel, A. (2002). Observed changes in seasons: An overview. *International Journal of Climatology*, 22(14):1715–1725.
- Winkler, S. (1980). Temperatur. In *Einführung in die Pflanzenökologie*, chapter Autökologi, pages 92, 101–103. Gustav Fischer Verlag, Stuttgart, 2 edition.

Appendix

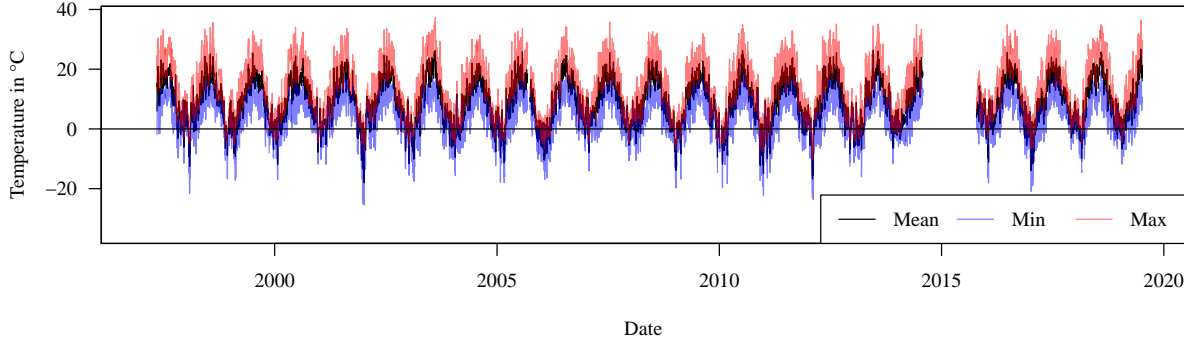


Figure 53: Daily Aggregated Temperature Data at 2 m height at the EBG Site over the entire measuring Period, measured with the HMP 45. The Daily Mean Temperature is shown in black, the Daily Minimum Temperature in blue and the Daily Maximum Temperature in red.

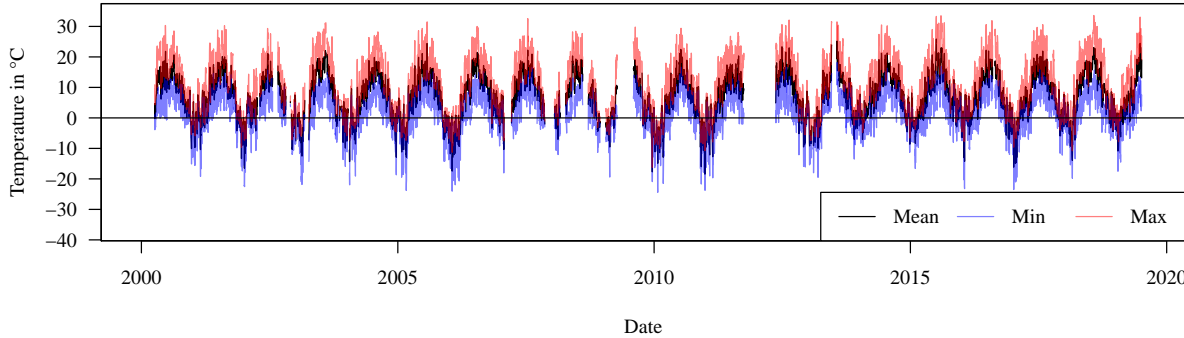


Figure 54: Daily Aggregated Temperature Data at 2 m height at the Voitsumra Site over the entire measuring Period, measured with the HMP 45. The Daily Mean Temperature is shown in black, the Daily Minimum Temperature in blue and the Daily Maximum Temperature in red.

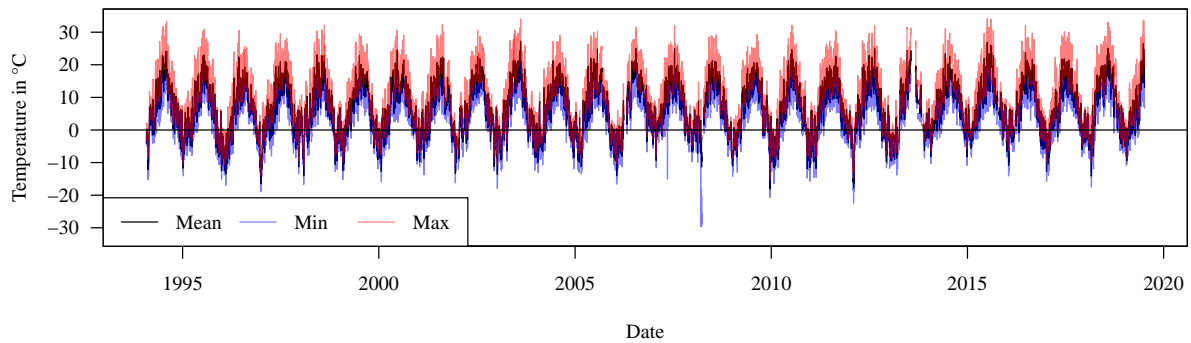


Figure 55: Daily Aggregated Temperature Data at 2 m height at the Waldstein Container Station over the entire measuring Period, measured with the HMP 45. The Daily Mean Temperature is shown in black, the Daily Minimum Temperature in blue and the Daily Maximum Temperature in red.

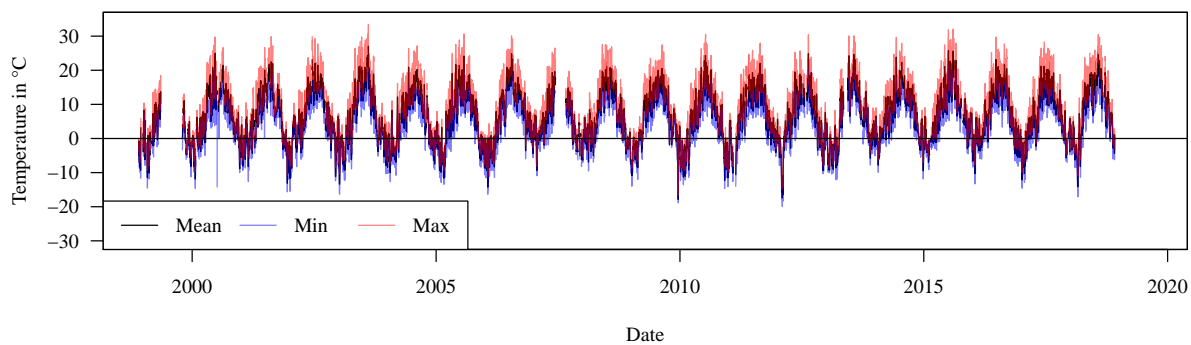


Figure 56: Daily Aggregated Temperature Data at 2 m height at the Waldstein Tower Station over the entire measuring Period, measured with the HMP 45. The Daily Mean Temperature is shown in black, the Daily Minimum Temperature in blue and the Daily Maximum Temperature in red.

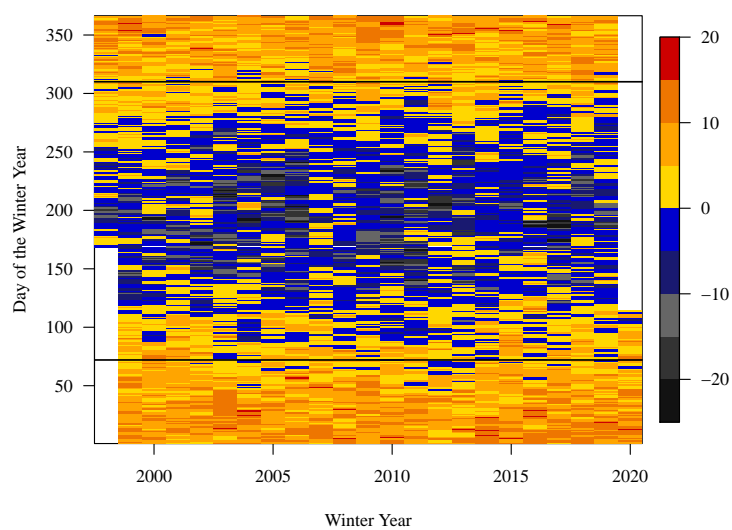


Figure 57: Hovmöller Plot of the Daily Minimum Temperature Data at the Voitsurma Station. All Frost Days (T_{\min} below 0°C) are depicted in blue. The Mean First and Last Frost Days are shown with two black Lines. Data Gaps are shown in white.

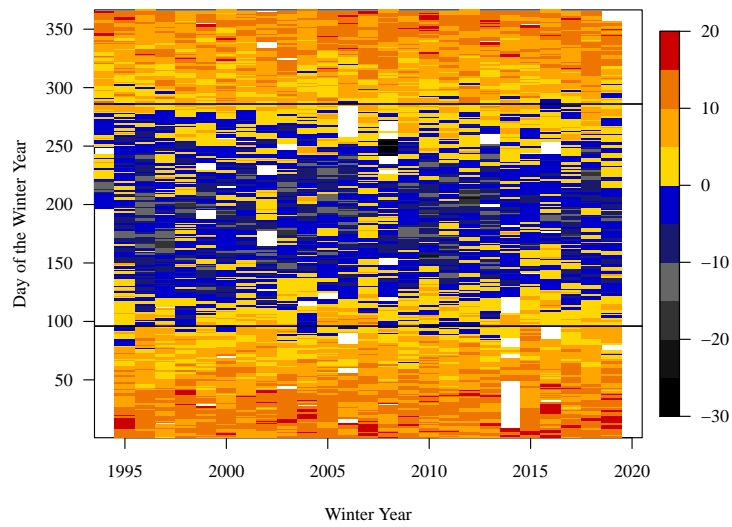


Figure 58: Hovmöller Plot of the Daily Minimum Temperature Data at the Voitsurma Station. All Frost Days (T_{\min} below 0°C) are depicted in blue. The Mean First and Last Frost Days are shown with two black Lines. Data Gaps are shown in white.

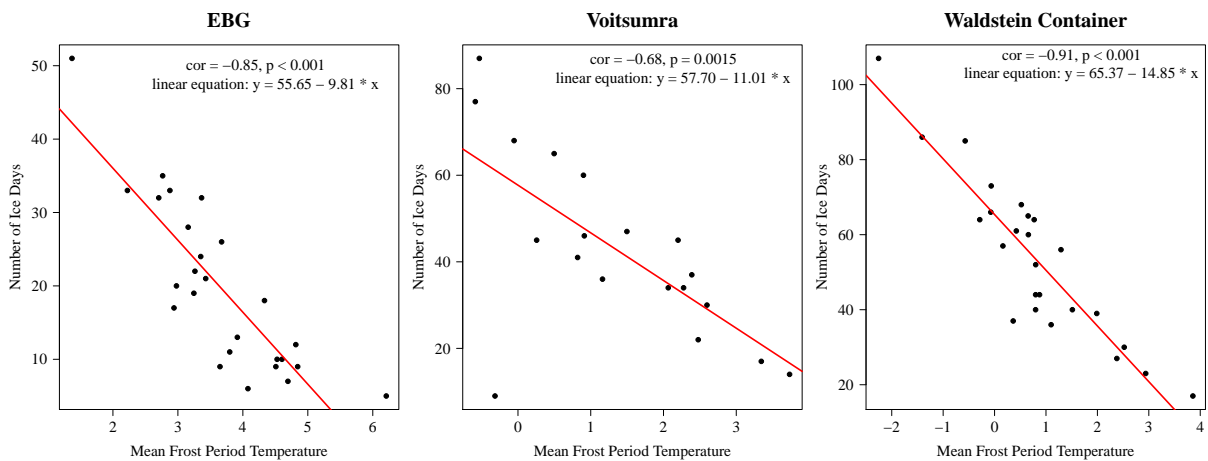


Figure 59: Scatterplot of the the Number of Ice Days versus Mean Frost Period Temperature at the EBG, Voitsurma and Waldstein site. A Linear Regression Line is shown additionally in red. The results of the Correlation Analysis and the Linear Equation are shown in the graphic.